BEHAVIOR OF MODEL FLEXIBLE PILES UNDER INCLINED LOADS IN SAND

MANOHAR S. RUPRAI

BEHAVIOUR OF MODEL FLEXIBLE PILES UNDER INCLINED LOADS IN SAND

BY

MANOHAR S. RUPRAI B. Eng.

© A thesis submitted to the School of Graduate Studies in partial fulfillment of the requirements for the degree of Master of Engineering

Faculty of Engineering and Applied Science
Memorial University of Newfoundland
July 1987

St. John's Newfoundland Canada

ISBN 0-315-39485-4

ABSTRACT

The increasing use of fixed offshore platforms supported by pile foundations has encouraged the development of more rational methods of analysis of piles subjected to combined axial and lateral loading. The combination of large lateral loads resulting from the action of wind, waves and currents in conjuction with vertical loads has created the need to analyze systems exposed to large inclined loads.

The scope of this thesis is to study the pile-soil interaction of a vertical flexible pile under inclined loadings in dense sand. To study the interaction, model flexible piles of 25 mm,42 mm and 60 mm diameters were jacked into sand with controlled density. These model piles were instrumented with load-cells and strain-gauge bridges to measure the bending moment distributions. The piles were tested under vertical, horizontal and inclined loads, using a computerized data acquisition system. A suitable soil container and laboratory test frame were assembled to conduct the tests.

The vertical load test results indicated that the value of the bearing capacity factor ,N_q , was constant with depth and consistently smaller than that predicted by various existing theories. The results also indicated that the piles had a critical depth where the point resistance became constant with depth, at a pile diameter/depth ratio of about 20.

Experimental p-y curves were compared with those proposed by Reese et al (1974), Matlock et al (1980), Scott (1980) and Parker (1970). The test data indicate that the semi-empirical methods underestimate the ultimate resistance near the pile head and overestimate it at depth. Computed response of piles under test conditions showed good agreement with the measured response.

The ultimate load capacity under inclined load decreases with load inclination, with a rapid reduction for load inclinations between 45 and 90 degrees. Compared to a pile subjected to only lateral load, the vertical load on the pile increases the lateral deflections by about 4 to 15 %, and the maximum moment in the pile section by about 8 to 16 % for load inclinations from 60 to 30 degrees.

ACKNOWLEDGEMENTS

This thesis was completed in the Faculty of Engineering and Applied Science at Memorial University of Newfoundland. The project was partially funded through an operating grant from the Natural Sciences and Engineering Research Council of Canada. The author wishes to acknowledge the receipt of a Memorial University Fellowship and a graduate supplement during the period of this study.

The author appreciates very much the advice, guidance, and careful review of the manuscript by his supervisor Dr.T.R. Chari, Professor and Associate Dean of Engineering. Thanks are due to Dr. G.R. Peters, Dean of Engineering for facilities provided and to Dr. F.A. Aldrich, Dean of Graduate Studies for his help and encouragement.

The author expresses his special appreciation to Mr. J. Joo for his help in the experiments. Thanks are also due to Mr. P. Robinson, Mr. J. Andrews and their colleagues at the University Technical Services for assembling the experimental facilities.

TABLE OF CONTENTS

LIST OF FIGURES

LIST OF TABLES

LIST OF SYMBOLS

The symbols in this thesis conform generally to the recommendation of the Canadian Geotechnical Society. They are also defined where they first appear in the text of the thesis.

A_p	Area of pile base (L^2)
A_s	Area of pile shaft embedded in the soil (L^2)
B	Diameter or width of pile (L)
C_u	Uniformity coefficient (dimensionless)
D	Depth of pile beneath ground (L)
D_n	n percent grain size (L)
D_r	Relative density of solids (dimensionless)(formerly specific gravity)
E	Modulus of linear deformation (FL^{-2})(modulus of elasticity)
E_s	Soil modulus,coefficient of subgrade reaction
e	eccentricity (L)
F	Factor of safety
H	Lateral force applied to a pile (F)
h	pile increment length (L)
I	Moment of inertia (L^4)
I_D	Density index (%)
K_a	Coefficient of active earth pressure (dimensionless)
K_o	Coefficient of earth pressure at rest (dimensionless)
K_p	Coefficient of passive earth pressure (dimensionless)
L	Length of pile (L)
M	Moment in a pile (FL)
N	S.P.T. blow count (Blows per 0.3m)

N_c	
N_q	Bearing capacity factors (dimensionless)
N_γ	
n_h	Horizontal coefficient of subgrade reaction (FL^{-3})
p	Soil resistance per unit length of pile (F/L)
$p-y$ curves	curves relating soil resistance to pile deflection
Q	Applied axial load (F)
Q_a	Ultimate axial load (F)
Q_n	Ultimate lateral load (F)
Q_p	Point resistance force (F)
Q_s	Total shaft resistance (F)
Q_s'	Total pull out resistance (F)
Q_u	Ultimate inclined load (F)
q_c	Static cone point resistance (FL^{-2})
q_p	point resistance pressure (FL^{-2})
q_{pn}	Net point resistance pressure (FL^{-2})
q_s	Unit shaft resistance (FL^{-2})
T	Stiffness factor (L)
w	Water content (%)
x	Coordinate measured along the pile axis (L)
y	Lateral pile deflection (L)
α	Inclination of load (deg)
γ	Unit weight (FL^{-3})
γ_d	Dry unit weight (FL^{-3})
δ	Angle of wall-soil friction (deg)
ν	Poisson's ratio for a soil (dimensionless)

ρ	Density (ML^{-3})
$\rho_{d(max)}$	Maximum dry density (ML^{-3})
$\rho_{d(min)}$	Minimum dry density (ML^{-3})
σ	Total normal stress (FL^{-2})
σ'	Effective normal stress (FL^{-2})
τ	Shear strength (FL^{-2})
ϕ	angle of internal friction (deg)

CHAPTER 1

INTRODUCTION

1.1 GENERAL

Pile foundations are frequently used for structures when the soil immediately below the base will not provide adequate bearing capacity. The purpose of the piles is to transfer the load from the structure to soil strata which can sustain the applied loads.

For vertical piles when the loads from the structure are vertical, then the loads transmitted to the piles will be principally axial. If some horizontal load component is present a lateral force will also be transmitted to the piles. For most structures both horizontal and vertical components of load are present. In some instances, the horizontal component will be small and can be neglected. However, for many structures such as offshore drilling platforms, quay and harbour structures, lock structures, and transmisson tower foundations, significant horizontal forces are likely to be produced either due to winds, or waves, or a combination of both. Therefore, for a complete analysis of a pile foundation for such structures, the behaviour of the piles must be analyzed for both axial and lateral loads.

When the axial and lateral load on a pile increase at a constant rate the applied load on the pile is inclined at some constant angle, α. Presently, the methods of analysis of piles subjected to inclined loads use the principle of superposition by considering the axial and lateral loads separately (Reese 1975, Matlock et al 1983). However, in case of long flexible piles, that are likely to cause the soil to yield, superposition will not hold good (Madhav et al, 1982). Hence, the pile has to be analysed using a combined analysis approach.

The increasing use of fixed offshore platforms supported by pile foundations has encouraged the development of more rational methods of analysis of piles subjected to combined axial and lateral loading. The behaviour of single piles under combined axial and lateral loads also forms an important input into the analysis of offshore pile groups (Poulos 1980, Toolan 1980).

Evans (1953) conducted one of the earliest experimental studies of vertical piles subjected to a constant vertical load with increasing horizontal load. Since then, investigation of piles subjected to inclined loads has been confined to small-scale rigid piles (Awad and Petrosovits 1968, Meyerhof and Ranjan 1972, Meyerhof et al 1981, 1983). Meyerhof et al (1981) have proposed an interaction equation for estimating the ultimate load under inclined loads for rigid piles. This equation was verified subsequently by Chari and Meyerhof (1983) using a larger 75 mm diameter model pile.

1.2 SCOPE OF THE INVESTIGATION

Published literature contains a considerable amount of information on piles subjected to axial or lateral load. However, there is limited data on piles, in particular long flexible piles, subjected to oblique (inclined) loads. Accordingly presented herein is a study of the behaviour of a flexible pile in cohesionless soil subjected to inclined loads. This study was carried in conjunction with a companion study on the behaviour of short rigid piles subjected to inclined loads (Joo 1985).

Laboratory facilities were designed and assembled for conducting model pile tests. Instrumented model piles of 25 mm, 40 mm, and 60 mm diameters were used. Laboratory tests on model piles provide data on the effect of load inclination on the load-displacement relationship and the ultimate pile resistance.

The specific objectives of this investigation are :

(1) to determine the variation in ultimate bearing capacity with varying inclination of the load,

(2) to determine the behaviour of laterally loaded piles and compare experimental p-y curves with theoretical curves, and

(3) to analyze and correlate the results with available theoretical and empirical methods.

A brief literature review is presented in Chapter 2. The failure mechanism of piles under axial and lateral loads together with the theories for determining ultimate bearing capacities are described. Chapter 3 contains a description of the laboratory facilities, instrumentation, and the types of experiments conducted. Analysis of the laboratory results, comparision of measured and predicted capacities, and the influence of different variables are analyzed in Chapter 4. Finally, the summary and conclusion from this investigation and recommendations for further work are presented in Chapter 5.

CHAPTER 2

REVIEW OF LITERATURE

2.1 GENERAL

Piles may be classified in several ways and into several categories. A summary of the major factors which govern the classification is given in Table 1. A definition diagram showing the commonly used nomenclature for piles is given in Figure 1.

Piles may be subjected to vertical loads, lateral loads, or a combination of both resulting in an inclined load. Vertical piles usually support structures carrying predominantly vertical loads and may also be used to resist uplift forces in marine structures. Lateral forces most frequently occur when the piles are required to restrain forces causing the sliding or overturning of structures. Lateral forces on land may be caused by earth pressure, wind, or earthquakes. In marine structures lateral forces may be caused by the impact of berthing ships, or by the action of wind, current, waves, and floating ice. Vertical piles have low resistance to lateral loads and raking or battered piles may sometimes be used to carry heavy lateral forces.

Piles subjected to lateral loads are classified as free-headed or restrained piles and as short, intermediate or long piles. A free-headed pile is free to rotate at its head. A restrained pile is fixed against rotation at its head by sufficient embedment of the pile head into the pile cap to develop a fixed end moment at the top of the pile.

Considerable research has been done in the past on the behaviour of axially and laterally loaded piles, but this research has not yet yielded any comprehensive method which can be universally applied to all types of soils or piles. This is

TABLE 1

Pile Type Classification

	Factor	Sub-group
1	Installation	Driven; bored; cast-in-place; jetted; excavated; augered;
2	Displacement	Displacement; low-displacement; non-displacement;
3	Material	Concrete; steel; wood;
4	Function	Shaft bearing; toe bearing;
5	Capacity	High; moderate; low;
6	Shape	Square; round; hexagonal; octagonal; H-section;
7	Environment	Land; marine; off-shore;
8	Inclination	Vertical; battered;
9	Length	Long; short;
10	Structure	Bridges; buildings; platforms; towers; machinery; etc.

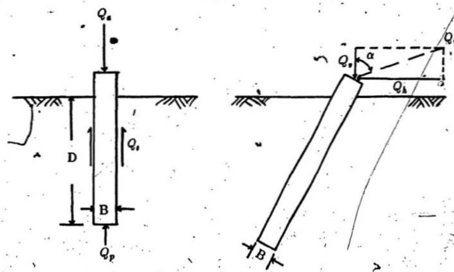

(a) A vertical pile under vertical loads

(b) A batter pile under inclined or lateral loads

NOMENCLATURE

B -diameter of pile

D -embedment depth of pile

D_o -depth of pile rotation point

E -modulus of linear deformation

e -eccentricity

H -applied lateral force

I -moment of inertia

n_h -horiz. coeff. of subgrade reaction

Q_a -applied axial load

Q_u -applied inclined load

Q_p -point resistance force

Q_s -total shaft-resistance

$Q_v = Q_u \cos \alpha$

$Q_h = Q_u \sin \alpha$

$T = \left[\frac{EI}{n_h}\right]^{1/5}$

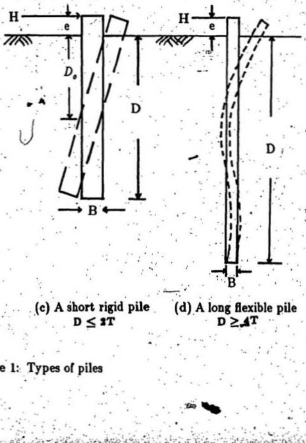

(c) A short rigid pile
D ≤ 2T

(d) A long flexible pile
D ≥ 4T

Figure 1: Types of piles

primarily due to the often highly variable and heterogeneous nature of natural soil deposits that causes their engineering properties to vary widely from point to point. Associated with this are the problems of testing representative soil samples from the construction site. Moreover, laboratory tests and methods of analysis do not often take into account the non-linear and anisotropic behaviour of soils, and empirical correction factors are used to account for real soil behaviour.

A number of bearing capacity theories, to estimate the ultimate vertical load capacity, have been developed for footings and pile foundations during the past fifty years. For sands most methods use the friction angle as the primary parameter for evaluating bearing capacity factors (Terzaghi 1943, Meyerhof 1951, Vesic 1963). However, there are other parameters such as pile size, depth of penetration, and density index of the sand which also influence the bearing capacity.

The lateral resistance of a pile is governed by either the yield strength of the pile or by the ultimate passive resistance of the supporting soil. Normally, for a short pile, the ultimate lateral load is governed by the passive resistance of the soil, whereas the strength of the pile section governs for a long pile. A pile of intermediate length should be checked for both modes of failure. The ultimate lateral load on vertical short rigid piles is generally computed based on lateral earth pressure theories (Brinch Hansen 1961, Broms 1964, Petrasovits et al 1972, Meyerhof et al 1981). Methods for predicting the lateral load behaviour of long flexible piles can be divided into elastic methods (Poulos 1971) and subgrade reaction methods (Broms 1972).

The ultimate resistance of piles subjected to inclined loads is a function of both the vertical and lateral load capacity. Yoshimi (1964) and Broms (1965) provide solutions to this aspect. Awad and Petrasovits (1968) showed the similarity between a batter pile subjected to vertical load and a vertical pile subjected to inclined load. Meyerhof et al (1981) presented an interaction equation to compute the ultimate capacity of rigid piles under inclined load. For flexible piles, the principle of superposition is usually used in making the assumption that there is no interaction between axial and lateral pile behaviour. Madhav et al (1982) however, state that in the case of long flexible piles, that are likely to cause the soil to yield, superposition will not hold good. Hence, the pile has to be analyzed using a combined analysis approach.

2.2 LONG VERTICAL PILES UNDER AXIAL LOADS

Piles usually receive support from both end bearing and shaft resistance. The relative magnitude of the shaft and base capacities will depend on the geometry of the pile and the soil profile. Piles which penetrate a relatively soft layer of soil to found on firmer stratum are referred to as end-bearing piles and will derive most of their capacity from the base capacity, Q_b. Where no firm stratum is available to found the piles on, the piles are known as friction or floating piles. In cohesive soils, the shaft capacity of a friction pile will often amount to 80-90% of the overall capacity, while in non-cohesive soils the overall capacity will be more evenly divided between shaft and base.

The ultimate bearing capacity of a pile , Q_u , is generally represented by :

$$Q_u = Q_b + Q_s = q_b A_p + f_s A_s \tag{1}$$

where Q_b - ultimate base load,

Q_s - ultimate side load,

q_b - ultimate unit bearing pressure,

f_s - ultimate unit side or friction resistance,

A_p - area of the pile base,

A_s - area of the pile shaft.

Successful application of the bearing capacity equation depends on the selection of the appropriate values of q_b and f_s. These must take into account the combined effects of soil conditions, pile type and dimensions, method of pile installation, and manner of loading.

The classicial theories of bearing capacity of piles are essentially based on the assumption that the soil is a rigid plastic material, while the effect of the compressibility of the soil is considered only empirically. It is also assumed that the cohesion and the angle of internal friction (c and ϕ) are constant regardless of the level of stress and strain. Most of the present day solutions are based on the selection of a plausible collapse mechanism in which the shear strength of the soil is fully developed along discontinuities, and considerations of the equilibrium of external and ~~internal~~ forces.

Research shows that the point and frictional resistance do not increase in proportion to depth, but remain relatively constant beyond a certain penetration depth, known as the critical depth, D_c (Kerisel 1964, Vesic 1964, Tavenas 1970, Hanna and Tan 1973).

Due to uncertainties in evaluating the bearing capacity factors, a number of codes or recommended practices have been developed which are based on experience. These codes or practices are developed for specific geographical areas or for specific pile type and uses. One example is the API recommended Practice for Planning, Designing and Constructing fixed Offshore Platforms (1982). This code uses the concept of critical depth and recommends limiting values for q_b and f_s based on local conditions.

The ultimate bearing capacity of a pile can be estimated by several methods and the most commonly used are :

(1) based upon bearing capacity theories ,

(2) from the results of in-situ penetration tests , and

(3) pile load tests.

2.2.1 POINT OR END BEARING RESISTANCE

According to Vesic (1967) most of the existing solutions for the problem of unit base resistance are the extensions of the classical work on punching failure by Prandtle (1921) and Reissner (1924). Caquot (1934) and Buisman (1935) applied these solutions to the problem of bearing capacity of deep foundations. Vesic (1967,1977) has summarized the various theoretical approaches for the failure mechanism of soil as shown in Figure 2.

Among the many contributors in this area of study were: Terzaghi, De Beer and Jaky in the 1940's; Meyerhof, Caquot and Kerisel in the 1950's; Brinch Hansen, Berezantsev and Yoroshenko, and Vesic in the 1960's. Skempton, Yassin and Gibson (1953) used a somewhat different approach treating the soil failure induced by the pile base as a special case of the expansion of a cavity inside a solid. Vesic (1977) used a similar approach and carried out a large scale experimental study.

In all of the theoretical solutions cited above, the ultimate unit base resistance q_b , is expressed by the following general expression:

$$q_b = cN_c + \gamma ' DN_q + \frac{B}{2}\gamma ' N_\gamma ' \qquad (2)$$

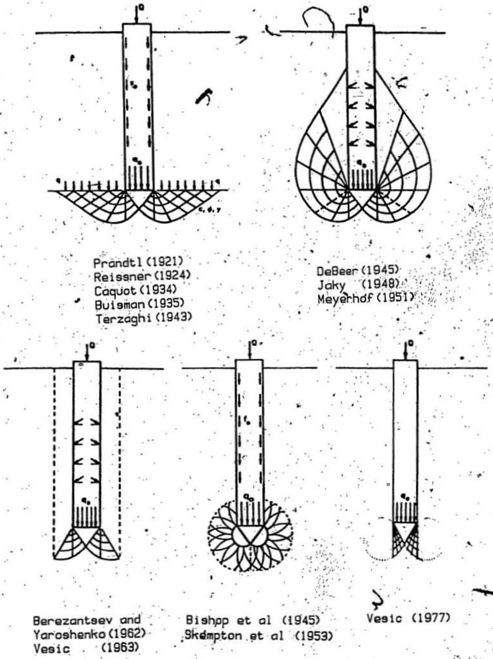

Figure 2: Assumed failure patterns of soil

where q_b is the ultimate unit base resistance,

N_c, N_q, N_γ are the bearing capacity factors,

B is the pile diameter,

γ' is the effective unit weight of soil at the pile tip,

c is the cohesive strength of soil, and

D is the vertical distance between the ground surface and the level of pile tip.

For cohesionless soils, the first term in this equation can be eliminated. For normal pile lengths D/B will be greater than 15 and the term involving B will be relatively small and can be neglected. Hence, Equation 2 can be simplified (Kezdi 1975, Vesic 1968, Coyle 1979) as:

$$q_b = \gamma' D \, N_q \tag{3}$$

All of the bearing capacity theories require the evaluation of N_q for use in Equation 3. Vesic (1967,1977) has summarized the values of N_q according to different theories as presented in Figure 3. It is evident that there are major deviations from one theory to another. Vesic (1967) and Nordlund (1963) have reported, that in practice the values of Brezantzev et al (1961) appear to best fit the available test data.

Kerisel (1964) and Meyerhof (1976) reported that the value of N_q in sand increases with depth and reaches its maximum value at less than half the critical depth D_c, which is discussed further. Durgunoglu and Mitchell (1973) found that N_q increases with increasing D/B ratio, while Vesic (1977) concluded that N_q is a constant independent of depth.

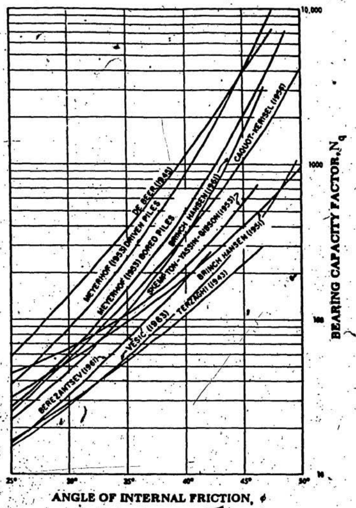

Figure 3: Bearing capacity factors for circular deep foundations after Vesic (1977)

Research by Kerisel (1961) and Vesic (1967) has revealed that the unit shaft and base resistances of a pile do not necessarily increase with depth, but instead reach almost constant values beyond a certain depth called critical depth, D_c. These characteristics have been confirmed by subsequent research (BCP Committee 1971, Tavenas 1971, Hanna and Tan 1973, and Meyerhof 1976). In loose sand, constant values were attained at L/B ratios of about 10 and, in dense sand of about 30.

This limiting value of end bearing has been attributed to some form of arching effect (Terzagh 1943). Fleming et al (1985) however, state that a more rational explanation lies in the variation of friction angle, ϕ', with confining pressure. Bolton (1984) discussed the strength and dilatancy characteristics of sand and showed that the bearing capacity of a deep strip footing becomes asymptotic towards a limiting value when the variation of ϕ' with confining pressure is allowed for. Fleming et al (1985) have used the same approach as Bolton to estimate the bearing capacity of deep circular footings.

Equation (3) is used with values of N_q recommended by Berezantzev et al (1961) as the design values. An appropriate value of ϕ' is then chosen based on the type of non-cohesive material, its relative density, and the average stress level at failure. Following Bolton (1984), ϕ' may be related to the relative density of the sand, corrected for the mean stress level, p', and a critical state angle of friction, ϕ'_{cv}, which relates to conditions where the soil shears with zero dilation (i.e. at constant volume). The corrected relative density, I_R, is given by

$$I_R = I_D(10 - \ln p') - 1 \qquad (4)$$

where I_D is the uncorrected relative density, and

p' is the mean effective stress in units of kN/m^2.

A lower limit of zero may be taken for I_R at very high stress levels, while values of I_R greater than 4 should be treated with caution. The appropriate value of ϕ' may then be calculated from

$$\phi' = \phi'_{cv} + 3I_R \quad (degrees) \tag{5}$$

The average mean effective stress at failure may be taken approximately as the geometric mean of the end-bearing pressure and the ambient vertical effective stress, i.e.

$$p' = \sqrt{(N_q)\sigma_v{}'} \tag{6}$$

The end bearing pressure q_b, may now be calculated, for given values of ϕ'_{cv}, I_D, and $\sigma_v{}'$ by iterating between equations (4) to (6), and the chart for N_q shown in figure 3. Fleming et al (1985) have presented charts of end bearing pressure against ambient vertical effective stress for different values of ϕ'_{cv} and I_D.

The process of pile driving into sand displaces the particles and changes the density of sand for some distance radially around the shaft and vertically beneath the base. The bearing capacity of a driven pile in sand depends very largely on the mean density of this disturbed zone (Vesic 1964). Poulos (1980) suggests that the value of ϕ should be taken as the final value subsequent to driving as given by Meyerhof and Kishida (1965) :

$$\phi = \frac{\phi' + 40^\circ}{2} \tag{7}$$

where ϕ' =angle of internal friction prior to installation of pile

Equation 7 implies that there is no change in density index for soils with an internal friction angle of 40° or greater.

Vesic (1977) has given the following equation for q_b

$$q_b = \frac{(1+2K_o)\gamma' D}{3} N_\sigma \tag{8}$$

where K_o is the coefficient of lateral earth pressure at rest,

γ' is the effective unit weight of soil,

D is the embedded pile length,

N_σ is the bearing capacity factor for mean normal stress and is a function of compressibility as well as internal friction angle of soil.

This method is a simple modification of the bearing capacity equation for base load to incorporate the fact that it is the mean normal ground stress rather than the vertical ground stress that governs base resistance.

2.2.2 FRICTIONAL OR SHAFT RESISTANCE

The unit skin friction for a straight-sided pile is the resistance to sliding of a rigid body relative to the surrounding soil. It is generally expressed as a function of the soil pressure acting normal to the pile surface and the coefficient of friction between the soil and the pile material. The unit shaft resistance of driven piles, q_s, in cohesionless soils at depth z below the ground surface can be calculated as follows (Meyerhof 1963, Nordlund 1963) :

$$q_s = K_s \sigma' \tan \delta \tag{9}$$

where K_s denotes the coefficient of earth pressure on the pile shaft,

σ' is the average effective overburden pressure at any point and is defined as the product of γ' and z,

δ is the angle of friction between the soil and pile material,

γ' is the effective unit weight of soil.

Equation 9 can be rewritten integrating along the embedded pile length for the total shaft resistance , Q_s , as follows:

$$Q_s = \frac{1}{2} K_s \gamma' D \tan\delta A_s \qquad (10)$$

where A_s is the total area of embedded pile shaft,

K_s is the average coefficient of earth pressure on pile shaft, and

D is the embedded depth of pile shaft.

Factors K_s and tan δ need to be established in order to determine unit skin resistance, and it is assumed that γ' and δ are constant along the length of the pile.

In the expression for skin friction for piles in sand the coefficient for earth pressure , K_s , is the most sensitive and also the most elusive factor. The magnitude of K_s , and therefore the pressure intensity, is known to be influenced by at least the following six factors (McClelland et al,1967):

(1) Initial state of stress (K_o) in the sand deposit,

(2) initial density of the sand,

(3) displacement volume of the driven or jacked pile,

(4) pile shape, including taper,

(5) installation procedures other than driving, and

(6) load direction (compression or tension).

However, for practical purposes averaged values of K_s can be taken for piles driven into sand. Suggested values for K_s for driven steel piles are 0.5 for loose sand and 1.0 for dense sand regardless of pile type and roughness of pile surface (Meyerhof 1951, Broms 1966, Coyle and Castello 1981). Fleming et al (1985) state that values of K_s vary in a similar fashion to N_q, and for full displacement, driven piles, K_s may be estimated from

$$K_s = N_q / 50 \tag{11}$$

Pontyondy (1961) determined the coefficient of friction using direct shear tests as 0.54ϕ for smooth steel piles and 0.76ϕ for rusted steel piles. Tomlinson (1981) quotes a value of skin friction angle δ as 20° for steel piles based on data from Broms (1966) and Nordlund (1965). Tomlinson also suggests that for piles deeper than 20 pile diameters average values of unit skin friction should be used based on the relative density of sand. Fleming et al (1985) suggest that the value of δ may be taken as the critical state angle of friction, ϕ'_{cv}, since no dilation is to be expected between the sand and the wall of the pile.

Because of the problem of obtaining undisturbed samples, the design parameters for piles in granular soils are usually obtained from the results of in-situ penetration tests.

2.2.3 DETERMINATION OF ALLOWABLE PILE LOADS FROM IN-SITU TESTS

In granular soils the values of both the end and skin friction resistance are extremely sensitive to small changes in the angle of friction, ϕ. It is possible to obtain reasonable estimates for both these parameters from in-situ penetration tests such as the standard penetration test (SPT) and the cone penetrometer test (CPT).

The bearing capacity of driven displacement piles in cohesionless soils can be estimated from the Standard Penetration Test as suggested by Meyerhof (1976) :

$$Q = mNA_p + n\bar{N}DA_s \tag{12}$$

where m is an empirical coefficient equal to 400 for driven piles and to 120 for bored piles,

N is the SPT index at the pile toe,

A_p is the area of pile base,

n is an empirical coefficient equal to 2 for driven piles and 1 for bored piles

$\bar{N}$ is the average SPT index along the pile,

D is the pile embedment depth, and

A_s is the pile unit shaft area.

The standard penetration test is subject to a multitude of errors and much care must be exercised when using the test results. The cone penetration test is considered to have greater accuracy than the standard penetration test.

A static penetrometer consists in principle of a conical tip which is pushed into the soil. Usually, the force is separated into end resistance and shaft resistance. The most advanced cone penetrometers measure separately the end resistance on the cone and the shaft resistance along a short section of the shaft near the end, called local friction. The use of the static cone penetrometer is presented comprehensively by Sanglerat (1972).

The ultimate bearing capacity of piles in cohesionless soils has been given by Meyerhof (1956) as :

$$Q = q_c A_p + 0.005 q_c A_s \tag{13}$$

where q_c is the average static cone point resistance,

A_p is the area of pile base, and

A_s is the area of embedded pile shaft.

The value of the cone end resistance has been used directly, without corrections, for the end resistance of a pile. It is also assumed that the unit shaft resistance is equal to 0.5% of the cone end resistance.

Nordlund (1963) recommends taking an average value of q_c over a depth range of 3 pile diameters above the pile base down to 2 diameters below the pile base. The end- bearing pressure is then taken as the average value of q_c . Fleming and Thorburn (1983) recommend more detailed schemes for averaging the cone readings, in order to give greater weight to the minimum values. The range over which the average is taken is extended up to 8 pile diameters above the level of the pile base. Thus, in homogeneous sand, end bearing pressure is estimated as

$$q_b = (q_{c\,1} + q_{c\,2} + 2q_{c\,3})/4 \qquad (14)$$

where $q_{c\,1}$ is the average cone resistance over 2 diameters below pile base,

$q_{c\,2}$ is the minimum cone resistance over 2 diameters below pile base, and

$q_{c\,3}$ is the average of minimum values lower than $q_{c\,2}$ over 8 diameters above pile base.

The static cone can be considered as an instrumented model pile pushed into the ground. The results enable the engineer to obtain a good estimate of the bearing capacity of a foundation pile. However, there are scale effects involved, and piles are normally driven and not pushed into the ground. Therefore, the pile capacity needs to be assessed by means of the bearing capacity equation adopting estimated values of various soil parameters where necessary and verified by pile load tests in the field.

2.3 VERTICAL FLEXIBLE PILES UNDER LATERAL LOADS

There are two theoretical methods for predicting lateral load behaviour of long piles :

(1) The elastic approach, which assumes the soil to be an ideal, elastic continuum.

(2) The subgrade reaction approach, in which the continuous nature of the soil medium is ignored and the pile reaction at a point is simply related to the deflection at that point.

2.3.1 ELASTIC METHODS

Lateral pile capacity can be calculated from Mindlin's equations (Mindlin, 1936) by assuming the soil to be an ideal, elastic, homogeneous, isotropic mass, having constant modulus of elasticity and a constant Poisson's ratio (Poulos and Davis, 1980). Most of the elastic analyses are similar in principle, the differences arising largely from details in the assumptions regarding the pile action.

A method of analysis for laterally loaded piles using Mindlin's equations was presented by Spillers and Stoll (1964). The behaviour was analyzed by replacing the lateral earth pressure along the pile by a series of point loads. Douglas and Davis (1964) have calculated from Mindlin's equations the pressure distribution, the lateral deflection and the rotation of laterally loaded vertical piles. Poulos (1971) used a similar approach replacing the laterally loaded pile by a thin rectangular strip with the same width and length as the pile. These strips were divided into a number of segments and the lateral earth pressure on each segment was assumed to be a constant. The Poulos solution is limited by its assumption that the soil modulus is constant with depth, whereas the modulus of elasticity usually increases for sand (Sogge, 1981). An approximate analysis for laterally loaded piles in soil, whose modul~~us increases with~~ depth was presented by Banerjee and Davis (1978).

Randolph (1981) derived expressions which allow the behaviour of flexible piles under lateral loading to be calculated, in terms of fundamental soil properties. The expressions are based on the results of finite element studies on the response of a laterally loaded cylindrical pile embedded in an elastic soil with stiffness varying linearly with depth. Charts have also been presented showing the deformed shape of the pile, and bending moment distribution down the pile, for an applied lateral load or moment at the pile head.

Horvath (1983) has used a simplified continuum approach based on simplified assumptions for vertical loads applied to the surface of the elastic continuum. The Young's modulus can be varied either linearly or with the square root of depth to more closely simulate the actual behaviour of the soil.

It is generally recognised (Morgan and Poulos 1968, Poulos 1973, Focht and Kocht 1973) that a linear analysis of the behaviour of laterally loaded piles has limited validity as the actual behaviour of laterally loaded piles is markedly non-linear. For application to problems involving real soils the elastic approach appears to be suitable for uniform deposits of cohesive soil where the elastic constants, E and ν could be expected to describe the behaviour. For sands, where they can usually be expected to vary with depth and stress level, the elastic approach does not give more accurate results than could be expected by the use of simpler methods based on subgrade reaction theory (Morgan and Poulos 1968).

2.3.2 SUBGRADE REACTION METHODS

These methods are based on an idealized model of the soil media proposed by Winkler (1867). It is assumed that the lateral earth pressure p on a pile increases linearly with increasing lateral deflection y according to the equation :

$$p = -E_s \, y \tag{15}$$

where E_s is the soil modulus or coefficient of subgrade reaction having units FL^{-3}.

The pile is regarded as being supported laterally by a series of independent linearly-elastic springs, so that deformation occurs only where loading occurs. Hence, the concept of a coefficient of subgrade reaction does not take into account the continuity of the soil mass (Poulos 1981).

The governing differential equation is derived on the assumption that the pile is a linearly elastic beam and that the soil reaction may be represented by a line load (Hetenyi 1946).

$$EI \frac{d^4y}{dx^4} - p = 0 \tag{16}$$

where y is the lateral deflection of the pile at point x along pile length,

p is soil reaction per unit length of the pile, and

EI is the pile flexural rigidity.

The effect of axial load on the pile is ignored, and substitution of Equation (15) into Equation (16) yields

$$EI \frac{d^4y}{dx^4} + E_s \, y = 0 \tag{17}$$

Solutions to the above equation may be obtained either analytically or numerically. Analytical solutions in closed form are only available for simple boundary conditions (Hetenyi 1946). Numerical solutions have been obtained using the finite difference method.

Palmer and Thompson (1948) first suggested the use of the finite difference method as a solution for free head piles. The mechanics of this solution was considerably simplified by Gleser (1954) and modified by Focht and McClelland (1955). Howe (1955) set up the solution on a computer which significantly reduced the solution time. Reese and Matlock (1956) extended the solution to introduce moment and shear as boundary conditions and produced a set of non-dimensional curves for the problem. A computer program was produced by Reese and Ginzberg (1958) in which the pile flexural rigidity could be changed abruptly at points along the pile length. The method was generalized by Matlock and Reese (1960).

Reese and Monoliu (1973) developed a computer program which uses successive difference equations based on reference to p-y curves for the particular soil. The soil modulus was determined at increments along the pile such that there was both compatibility and equilibrium for the soil, the pile, and the superstructure. The program has the advantage of analyzing laterally loaded piles subjected to both horizontal and vertical loading with different boundary conditions. Details of the program are documented by Reese (1975,1977).

Yakoyama (1985) has proposed the use of a non-linear differential equation of the second order, which was derived as an approximate form of a non-linear differential equation of the fourth order (equation 17). The major advantage of this method is that computational time required is significantly less than that for the fourth order equation and finite difference expressions of the second order equation can be obtained without any iterative procedures.

The earliest methods for analyzing laterally loaded piles were based on methods where the soil is in a state of failure under ultimate horizontal pressure. The best known of these methods are those provided by Brinch Hansen (1961) and Broms (1964). Broms calculated the ultimate lateral resistance and lateral deflections at working loads. Lateral deflections have been calculated using the subgrade reaction theory based on a simplified soil-resistance distribution along the pile.

Muzas (1972) calculated lateral deflections using the method of successive approximations by using a coefficient of subgrade reaction which is either constant or increases exponentially with depth. A similar approach has also been used by Mustafayev et al (1972). The results can be expressed in non-dimensional charts for both cases.

Mori (1964), Reddy and Valsangkar (1970), Reddy and Ramaswamy (1971,72 and 73), Madhav et al (1971) and Valsangkar et al (1973) have solved the differential equations given above for elasto-plastic soils when load-deformation consists of two straight lines. Reddy and Valsangkar (1970) presented the results in a non-dimensional form for the cases when the coefficient of subgrade reaction below the plastic zone is either constant or increases linearly with depth.

2.4 SOIL RESPONSE IN THE SUBGRADE REACTION METHODS

The modulus of subgrade reaction has been used extensively in solving the laterally loaded pile problem in spite of it not taking account of soil continuity. The simplicity of the model, availability of chart solutions, and ease of hand calculation favour its use to this day (Sullivan 1979, Hovarth 1984).

However, it has long been recognized that the behaviour of laterally loaded piles is frequently non-linear because failure of near surface soil develops under relatively low load levels. Ignoring the nonlinearity of the soil response may lead to conservative linear predictions in variance with actual behaviour (Ismael and Klym 1978). Probably the best known approach to overcoming this shortcoming has been the development of p-y curves.

2.4.1 THE p-y CURVES CONCEPT

A p-y curve is simply a nonlinear pressure versus deflection curve that is calculated a priori for a finite number of points along a pile. These curves substitute for the linear springs of the Winkler model, and are commonly determined using the strength deformation properties of the soil as obtained from standard laboratory tests.

The concept of p-y curves was first proposed by McClelland and Focht (1958), who attempted to correlate the horizontal reaction-deflection curves for the soil with stress-strain results from triaxial tests. An instrumented pile was used to obtain the pile reaction-deflection curves at various depths. Subsequently, Matlock 1970, Reese et al 1974, and Sullivan et al 1980 have followed similar procedures in determining p-y curves from field tests on fully instrumented piles, which have been standardized as their application is fairly simple.

The concept of p-y curves is defined in figure 4 (Reese and Cox 1969). Figure 4(a) shows a section through a deep foundation at some depth x_i below the ground surface. Before any lateral load is applied to the pile, the pressure distribution will be similar to that shown in figure 4(b). The resultant force obtained by integrating the pressure around the pile segment, in this case, will be zero. The deflection of the pile through a distance y_i at depth x_i generates the pressure distribution shown in figure 4(c). Integration of the soil stresses yields an unbalanced force p_i per unit length of pile. The same procedure may be applied

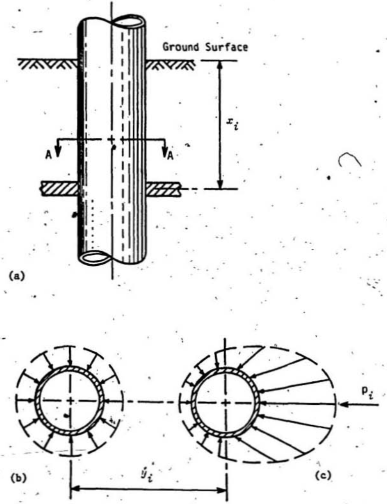

Figure 4: Graphical definition of p and y: (a) side view; (b) A-A, earth pressure distribution prior to lateral loading; (c) A-A, earth pressure distribution after lateral loading (Reese and Cox, 1969)

for a series of forces which may be combined into a p-y curve. In a similar manner, p-y curves for any depth may be defined, resulting in a series of p-y curves.

The curves seem to imply that the soil resistance for a given lateral deflection at a point is independent of the deflections at all other points. That assumption, of course, is not strictly true. However, experiments indicate that the soil reaction at a point is dependent essentially on the pile deflection at that point, and not on pile deflections above and below (Reese 1975).

2.5 METHODS FOR THE CONSTRUCTION OF p-y CURVES IN COHESIONLESS SOILS

The analysis of laterally loaded piles using p-y curves to represent the soil makes possible relatively simple and straight forward computations of pile-head flexibility and of stresses along the pile. Complete and comprehensive theoretical derivations of p-y curves from basic soil properties has not yet been developed because of complex stress conditions developed in the soil during installation and subsequent loading of the pile.

Four semi-empirical procedures for construction of p-y curves in cohesionless soils have been developed by Reese et al (1974), Matlock et al (1980), Scott (1980) and Parker (1970). Each was developed to fit data from a particular lateral load test or a specific set of tests on similar soils. The four procedures, denoted method A to method D, respectively are described briefly below.

2.5.1 METHOD A

Method A is the recommended procedure by the American Petroleum Institute (1982) which is basically the same as the procedure by Reese et al (1974) who describe it in detail. Data and subsequent correlation are based on a field pile load test reported by Cox et al (1974).

p-y curves are constructed for desired depths. Each curve consists of three segments : two straight lines and a parabola between as shown in figure 5. The value of K (N/m^2), the initial slope, is determined by multiplying k (N/m^3) times depth, where k is a modulus of lateral soil reaction. The ultimate soil resistance p_u is determined from the lesser value given by Equations 18 and 19, modified by an empirical adjustment parameter, which differs for static and cyclic loading and varies with pile diameter and depth.

$$p_u = \gamma z \; [\, D \,(K_p - K_a) + zK_p \tan\phi \tan\beta \,] \tag{18}$$

$$p_u = \gamma Dz \; (K_p^3 + 2K_o K_p^2 \tan\phi + \tan\phi - K_a) \tag{19}$$

where p_u is the ultimate soil resistance per unit of depth,

z is the depth below ground surface, D is pile diameter.

γ is the unit weight of the soil,

K_a is the Rankine active coefficient,

K_p is the Rankine passive coefficient,

K_o is the earth pressure coefficient,

ϕ is the angle of internal friction, and

$\beta = 45° + \frac{\phi}{2}$

The value of p_m (beginning of second linear segment of curve) is a certain percentage (determined from empirical charts) of p_u, while the values of y_m and y_u are ratios of the pile diameter. The point y_k, p_k is determined from an empirical relationship involving y_m, y_p, p_m, and p_u. The procedure is somewhat complicated to apply manually and can be programmed for efficient development of p-y curves.

2.5.2 METHOD B

Method B, a modification of the API method, was introduced by Matlock and Lam (1980). By realizing that some terms in the formulation of p_u can be taken as constants with little error, they were able to simplify Method A.

The ultimate soil resistance is calculated in the same way as in Method A, except that the terms have been grouped to form constants which vary with ϕ, as shown in Equations 20 and 21 :

$$p_u = (C_1 z + c_2 D)\gamma z \qquad (20)$$

$$p_u = c_3 D \gamma z \qquad (21)$$

The parameters C_1, C_2 and C_3 are evaluated from figure 6.

The p-y curves otherwise are the same as for Method A. Charts with non-dimensionalized values of p for corresponding values of y have been developed to make it unnecessary to calculate the p values from the different segments of the figure 5 curve. The deflections are chosen to give the critical points on the Method A curve. Note that it is not necessary to compute K. As with Method A, Method B sets p_u as the limit on the resistance of the soil to lateral deflection.

2.5.3 METHOD C

Method C was formulated by Scott (1980) who performed centrifuge tests on model piles in sand. It differs from the previous criteria in at least two important aspects. First the p-y curve is idealized by two straight line segments, which simplifies the calculations involved. The initial segment of the curve is similar to the other methods, because a subgrade modulus k times the depth z defines the

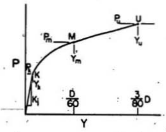

Figure 5: Method A p-y curve

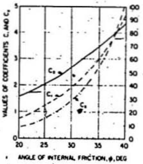

Figure 6: Factors for Method B

slope. The other segment is empirically assigned a slope of $\frac{kz}{4}$, which highlights the second difference from the other two methods. Because the upper segment has a constant non-zero slope, the method assumes that as the deflection increases , the soil resistance increases linearly with no limit. The ultimate soil resistance concept is therefore not applied.

The force per unit length p_k that exists at the beginning of the quasi-plastic line segment is given by :

$$\Omega = \frac{\sigma_o' D}{p_k} = \frac{1}{\pi}\left(\frac{1}{\sin^2\phi} + \frac{1}{3-4\nu}\right)^{0.5} \tag{22}$$

where σ_o' is the effective lateral stress in the soil,

p_k is the force per unit length at the beginning of quaso-plastic range,

D is the pile diameter,

ϕ is the angle of friction of the soil, and

ν is the Poisson's ratio of the soil.

Values of $\frac{1}{2}\sigma_o' D \,/\, p_k$ are graphed in figure 7. The corresponding displacement at the beginning of the quasi-plastic range is given by :

$$y_k = \frac{p_k}{E_s} \tag{23}$$

where $E_s = kz$.

The complete p-y curve is shown in figure 8.

2.5.4 METHOD D

Method D was originally formulated by Parker (1970) from his study of small diameter pipe piles and reformulated by O'Neill and Murchison (1983).

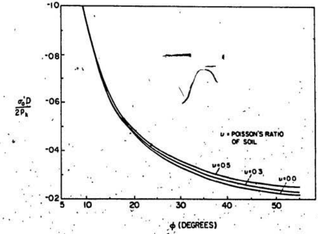

Figure 7: Design curve for Method C

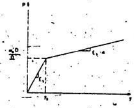

Figure 8: Method C p-y curve

The continuous hyperbolic tangent function is ~~used to~~ describe the p-y curves. The equation for the p-y curve is:

$$p = \eta A p_u \tanh\left[\left(\frac{kz}{A\,\eta p_u}\right)y\right] \qquad (24)$$

where p_u is the unmodified ultimate soil resistance (Equations 18 and 19).

The empirical adjustment factor A is :

A = 0.9 for cyclic loading,

A = 3 to 0.8z/D $\geq$ 0.9 for static loading,

η is a factor used to describe pile shape, taken to be 1.0 for circular prismatic piles,

kz is the product of lateral subgrade modulus and depth as used in Method A.

This method also provides for a limiting value of p.

Each of the above semi-empirical procedures was developed to fit data from a particular lateral load test or a specific set of tests on similar soils. No studies have been conducted to assess their universal validity. Reese et al (1974), Matlock et al (1980) and Parker's (1970) methods use the concept of limiting ultimate soil resistance, where as Scott's (1980) method assumes that the soil resistance increases linearly with no limit. Parker (1970) and Scott's (1980) methods are the simplest to use since they use a single function to describe a p-y curve.

2.6 INCLINED LOADS ON PILES

Piles under inclined loads or under combined axial and lateral loads are usually analyzed using the principle of superposition. It is assumed that the axial-load transfer characteristics are independent (uncoupled) from the lateral-load transfer characteristics. Thus, the axial and lateral behaviour of a pile can be studied and analyzed seperately. However, the effect of axial load on the lateral behaviour of a pile can be considered without violating the assumption of independence of soil behaviour. The modification of Equation (17) to include an axial force results in the equation

$$EI \frac{d^4y}{dx^4} + P_z \frac{d^2y}{dx^2} + E_s y = 0 \tag{25}$$

where P_z is the axial load on the pile.

Equation (25) is the desired equation for a laterally loaded pile considering the effect of an axial load and can be solved numerically using the finite difference method (Reese 1975). This equation, however does not give the deflection of the pile in the direction of the resultant load when the axial load is increasing in constant proportion to the lateral load. Madhav et al (1982) also state that in the case of long flexible piles, that are likely to cause the soil to yield, superposition will not hold good. Hence, the pile has to be analyzed using a combined analysis approach.

Most of the present day investigations for piles subjected to inclined loads have been based mostly on laboratory research in which small diameter rigid piles have been examined. Yoshimi (1965) and Broms (1965) provide solutions to pull out tests. Awad and Petrasovits (1968) showed the similarity between a batter pile subjected to vertical load and a vertical pile subjected to inclined load. Their experimental results indicated that the ultimate bearing capacity was a maximum for a load inclination of 22.5° and 16 to 35% higher than the ultimate vertical bearing capacity.

Meyerhof and Ranjan (1972), Meyerhof et al (1981,1983) have studied extensively the behaviour of small diameter rigid piles in the laboratory. They reported that the ultimate bearing capacity of vertical rigid piles under inclined loads decreased with the inclination of loads. Meyerhof et al (1981) have proposed an interaction equation for the determination of ultimate bearing capacity as follows :

$$\left(\frac{Q_u \cos(\alpha)}{Q_a}\right)^2 + \left(\frac{Q_u \sin(\alpha)}{Q_n}\right)^2 = 1 \qquad (26)$$

where Q_u represents the ultimate bearing capacity of the pile under inclined loads,

Q_a denotes the ultimate axial load of the pile,

Q_n is the ultimate lateral load of the pile, and

α is the inclination of applied loads to vertical in degrees.

Chari and Meyerhof (1983) have subsequently confirmed these results with a relatively larger pile of 75 mm diameter. The results indicated that there was good agreement between predicted and experimental results, and that the ultimate bearing capacity of the pile under inclined loads decreased continuously with increasing inclination of load.

Ramasamy et al (1982) have studied the behaviour of partially embedded piles with a considerable free standing (unsupported) length subjected to vertical and lateral loads based on the subgrade reaction theory. Series solutions to the governing differential equations show that the vertical load can increase the lateral deflection to an extent of about 7 to 16% depending on the degree of fixity of the pile head.

Madhav et al (1982) have modeled an axially and laterally loaded pile with an overhang similar to an offshore pile using the elastic continuum approach. The results have been compared with that of a pile acted upon by only lateral loads. The comparisons indicate that the lateral displacements increase with axial load due to the increased moments from the axial load and the corresponding yield of soil over a larger depth. Increase in the height of overhang also increases the lateral deflections.

A review of literature shows that there is a scarcity of experimental data on the behaviour of vertical flexible piles under inclined loads. Most of the existing experimental and analytical work is on the behaviour of rigid piles. An agreement or relationship between the ultimate capacity of flexible piles and load inclination does not seem to exist at present. This behaviour of flexible piles is examined in this thesis in some detail and the results thereof presented in Chapter 4.

CHAPTER 3

EXPERIMENTAL PROGRAM

3.1 GENERAL

The behaviour of flexible piles has generally been derived from a particular load test or a specific set of tests on similar soils. While model studies of axially loaded piles [redacted] common, few studies have been conducted to assess the validity of the semi-empirical methods describing the lateral load behaviour of piles. Laboratory tests on model flexible piles are sparse, especially for test piles instrumented with strain gauges and load cells. In this study, circular piles of 25 mm, 42 mm and 60 mm diameter embedded in sand, were tested under vertical and inclined loads in sand. For all the pile sizes the corresponding lengths of embedment were chosen to ensure that the piles behaved as flexible piles.

The test program was divided into the following three broad categories :

(1) Axial load tests to measure both the vertical and pull-out resistance of the piles,

(2) lateral load tests to determine the load-deflection behaviour of the piles together with the bending moment distribution in the pile shaft. Experimental p-y curves were derived and compared with theoretical p-y curves, and

(3) inclined load tests to determine the variation of ultimate bearing capacity of a pile with varying inclination of load.

To accomodate the physical size of the piles and the associated large forces, the soil container and the loading frame as shown in Figure 9 had to be suitably designed. Two screw jacks, with capacities of 178 kN and 44.5 kN with travel arms of 1.4 m and 0.35 m respectively were used in this study. The initial placement of the pile was done by jacking the pile vertically down using the larger screw jack. After jacking to the required depth, testing of the piles was done using the smaller jack with a swivel joint as shown in Figure 10.

A total of twenty tests were conducted in the experimental study. The design of the experiments and the experimental procedures are briefly discussed in the following sections.

3.2 TEST FACILITIES

The test facilities consist of a circular corrugated steel tank container for the soil, instrumented model piles, the loading frame and loading system, and the data acquisition unit. Views of the experimental set-up are shown in Figures 9 and 10. A detailed description of the various components is given below.

3.2.1 SOIL CONTAINER

A galvanized corrugated steel pipe 1.83 meters in diameter, 2 meters high with a wall thickness of 2.8 mm was used as the soil container in which the soil samples can be prepared under controlled conditions.

The minimum dimensions of the container are governed by the zone of soil influence around a pile pushed into the soil. The dimensions should be large enough to avoid end effects of the container with reasonable clearence. Figure 11 shows a typical pile pushed into sand with the zone of densification that develops around it. Table 2 is a summary of the published data on this phenemenon. The magnitude of dimensions a and b depend on the pile diameter, method of pile installation, and the density of sand.

The size of the soil container and the maximum size of the model piles was so chosen that there was adequate clearence to perform cone penetrometer tests

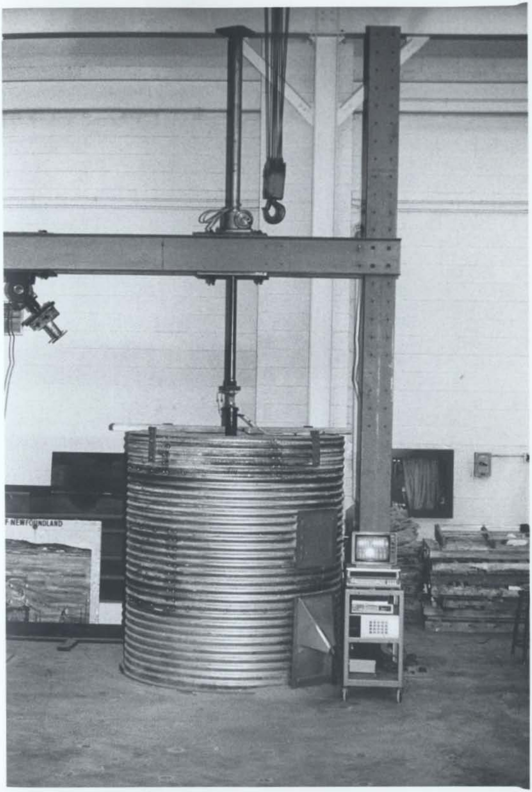

Figure 9: General experimental set up

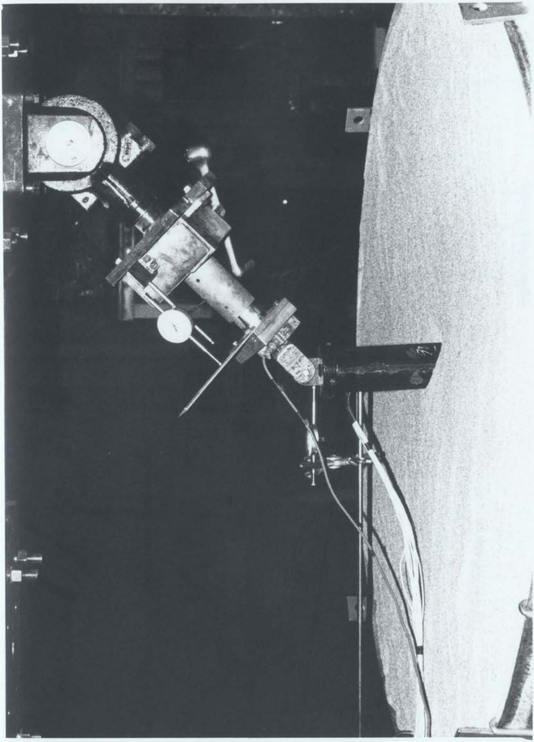

Figure 10: Configuration of loading system

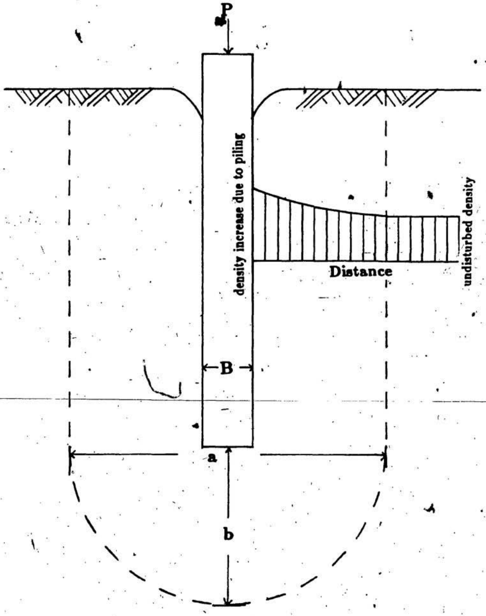

Figure 11: Influence zone of densification during placement of a pile

TABLE 2

Densification influence zone for driven pile in sand

INVESTIGATOR	DENSITY	INFLUENCE ZONE	
		a	*b*
Meyerhof (1959)	loose	6B-8B	5B
Kerisel (1961)	dense	5B	
	General		3B
Robinsky & Morrison (1963)	loose	7B-9B	2.5B-3.5B
	medium	10B-12B	3B-4.5B
Kishida (1963,1967)	loose	6B-8B	
	General		5B
Broms (1966)	General	7B-12B	3B-5B
Lamb & Whitman (1969)	General		16B

a represents the width of densification zone.

b denotes the depth of densification zone below the tip.

B is the diameter of pile.

on the relatively undisturbed soil outside the zone of influence, after the pile is tested.

The soil container has two side openings to facilitate easy removal of the soil after testing. The container rests on a heavily reinforced concrete floor and can be maneuvered easily between the loading frame by using an overhead crane.

3.2.2 LOADING FRAME

The loading frame was designed and fabricated using two W250 x 115 H sections for columns and a horizontal member made out of two C 310 x 31 channel sections as shown in figure 9. The overall size of the loading frame is 5.48 m high x 3.95 m wide. This frame is capable of withstanding vertical loads of 653 kN with a safety factor of 2 and horizontal loads of 16 kN applied 2.1 m from the base of the frame.

3.2.3 MODEL PILES

The major consideration was that the piles behave as an infinitely long flexible member rather than as a short rigid unit. The pile rigidity is described by the stiffness factor T which is expressed as (Davison and Parkash 1963, Broms 1964, Tomlinson 1977) :

$$T = \left(\frac{EI}{n_h}\right)^{1/5}$$

where EI is the stiffness of the pile, and

n_h is the coefficient of horizontal subgrade reaction.

The length of the pile has to be greater than 4T for behaviour as a long elastic pile and less than 2T for behaviour as a short pile. In designing the model piles, the values of coefficient of horizontal subgrade reaction obtained by Reese et al (1974) were used.

All the model piles were fabricated from standard seamless steel pipes. The pipes were split longitudinally and reassembled using suitably designed internal connecting rings to fasten the two halves. For purposes of pile stiffness computations, the values of EI for the piles were determined experimentally. A load cell was mounted at the bottom of the pile and strain gauges were placed at different points along the inside edge. Figures 12 and 13 show the model piles and their details. The physical properties of the piles are listed in Table 3.

3.2.4 INSTRUMENTATION AND DATA ACQUISITION SYSTEM

In the test program, during each test, the applied load, top deflection, and bending strains along the length of the pile shaft were continuously monitored.

The applied load was measured using a commercially available load cell. The load itself was applied either using a 1.4 m screw jack or a hydraulic jack, depending on whether the load was axial or inclined. The vertical end resistance of the pile was measured using a full strain gauge type load cell fabricated in-house. Figures 14 and 15 give the detail of the load cells. Displacements of the pile head were measured using linear variable differential transformers (LVDT) and dial gauges.

Electrical resistance strain gauges were used to measure bending strains. The gauges were Micro-Measurements Type EA-06-125BT-120, Option W, 120 ohm, gauge length 3.2 mm, and gauge factor 2.05. To install the gauges, the gauge locations were marked on the inside surface of each split half of pipe and thoroughly cleaned. Two strain gauges with their axes parallel to the axis of the pipe, were mounted on each half of the pipe at each gauge level. Lead wires were attached and the gauges were covered with waterproof coating for protection. The assembly is shown in figure 16. The lead wires were carried to the top end of the pipe and connected to the data acquisation unit through a hole in the pipe wall. The strain gauges at each level were connected in a full bridge circuit in order to give maximum sensitivity to bending. The gauge locations and bridge arrangement are shown in figures 13 and 17.

The output from the load cells, the LVDT's and the strain gauge bridges were recorded on magnetic tapes through an HP 86 micro-computer and on HP 3497A Data Acquisition/Control Unit. The required computer programs were developed for running the experiments and for subsequent plotting and analysis of data. Typical computer programs developed in this research are listed in Appendix A.

3.3 DETERMINATION OF THE PILE STIFFNESS

For the calibration of the strain gauges and to determine the pile stiffness, the pile was arranged as a simply supported beam with supports at the two ends. Loads were applied by placing known weights on the beam. The signals from the strain gauges were measured with the HP system described previously. Bending moments were computed from the known loads and points of application. Figure 18 is a typical calibration curve and the slope of the curve is the calibration constant for the strain gauge bridge.

The calibration constants used in the data reduction were the averages of the three values from different load configurations. The calibration constant for a particular location was multiplied by the output from the gauges at that location to obtain the bending moment in the pile.

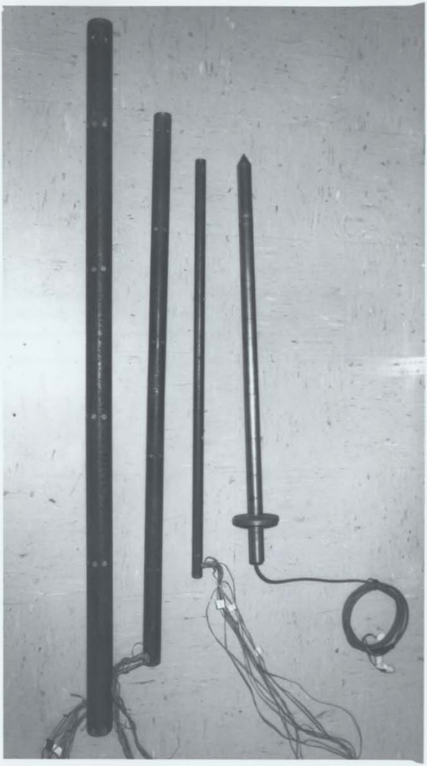

Figure 12: Model Piles

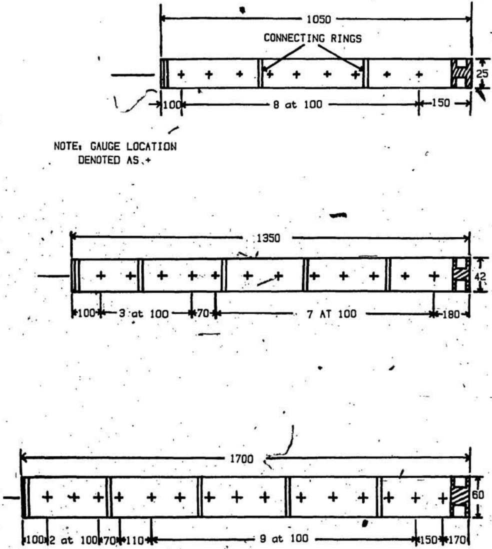

Figure 13: Details and dimensions (in mm) of piles

TABLE 3

Specification of Model Piles

PARAMETER	PILES		
Pile width, B (mm)	25	42	60
Length, L (mm)	1050	1350	1700
Thickness, t (mm)	2.87	3.6	4.8
Pile Stifness, EI (Nm^2)	810	5980	35260
Hor. coeff. of subgrade reaction for dense sand, n_h, (MN/m^3)	20	20	20
Min. embedded length for a long pile, L (mm)	800	1200	1500
Embedded length, D (mm)	1000	1300	1650

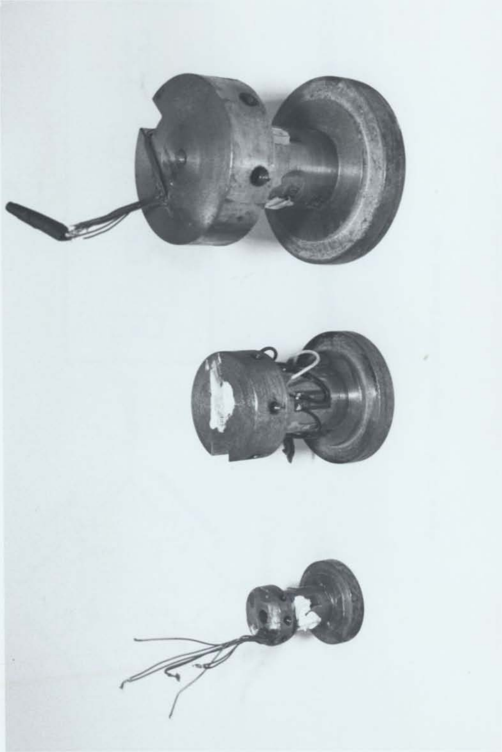

Figure 14: Load cells

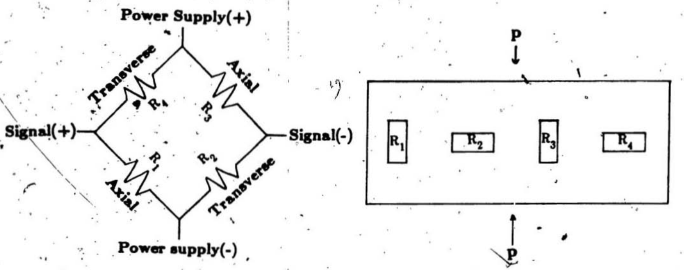

<CIRCUIT>

<DEVELOPED SURFACE WITH GAUGES>

Figure 15: Strain-gauge assembly for load cells

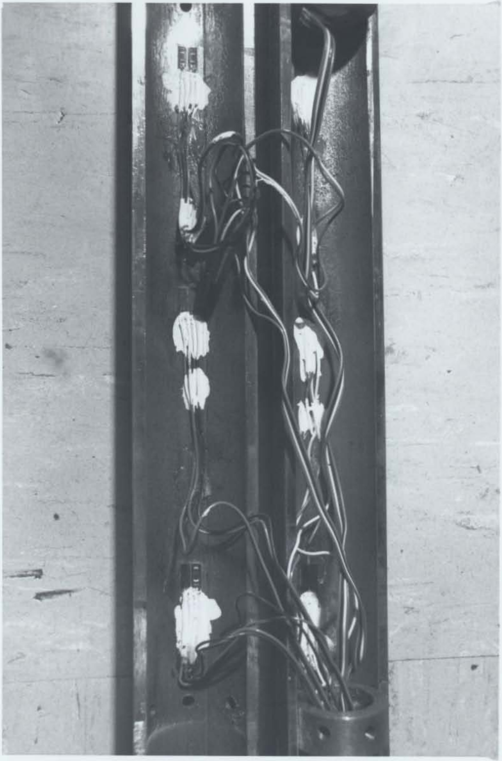

Figure 16: Pile cross section

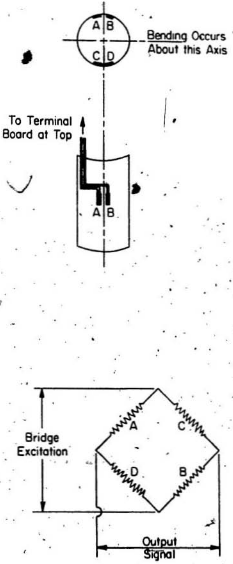

Figure 17: Strain-gauge bridge arrangement

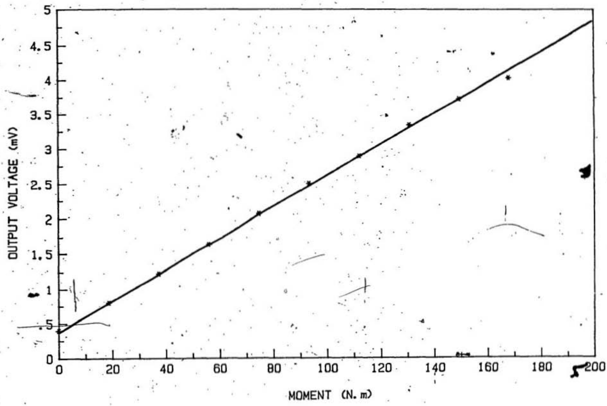

Figure 18: Example moment calibration constant determination

3.4 PROPERTIES OF SAND

The sand used was commercially available dry coarse silica sand. The grain size distribution illustrated in figure 19 indicates a uniform coarse sand. The general properties of the sand are listed in Table 4. The maximum and minimum dry densities obtained in the laboratory were 1570 kg/m^3 and 1340 kg/m^3, with a uniformity coefficient of 1.4. The sand bed used in the tests had a density of 1510 kg/m^3 with a density index of 0.77.

Direct shear tests and triaxial tests were performed on sand samples at a density of 1510 kg/m^3. An average internal angle of friction of 41.2° was obtained as illustrated in figures 20 and 21.

3.4.1 PREPARATION OF SAND BED

In the preparation of the sand bed in the container, the most uniform placement was obtained by the raining technique. The technique has been described by Bieganousky and Marcuson (1976) and also by Vesic (1965,1968). A single hose hopper was used as shown in figure 22. The height of free fall and rate of deposition was controlled to produce the desired density.

The sand was dropped through a flexible corrugated hose of diameter 50 mm with a 38 mm diameter 510 mm long straight plastic pipe at the open end. The free fall height was kept approximately constant at 100 mm and the sand laid in layers of 25 mm thickness to obtain the desired density of 1510 kg/m^3. Each hopper load of sand was weighed before pouring. The actual density as placed was computed by measuring the height of sand in the container by means of measuring scales along the inside wall of the container for each hopper load. The uniformity of density over the entire depth of soil was verified by cone penetrometer tests and also by the point resistance force during pile jacking.

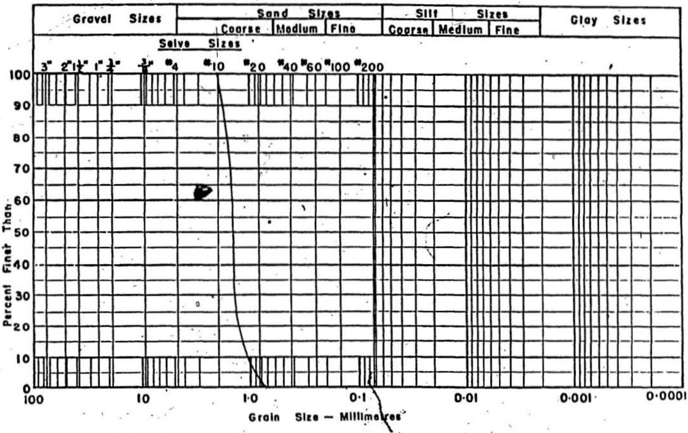

Figure 10: Grain-size curve

TABLE 4

Properties of sand used

PARAMETER	QUANTITY
Maximum dry density, $\rho_{d(max)}$	**1570 kg/m^3**
Minimum dry density, $\rho_{d(min)}$	**1340 kg/m^3**
Apparent density, ρ	**1510 kg/m^3**
Density index, I_d	**77%**
Apparent angle of internal friction, ϕ	**41.2°**
Effective grain size, D_{10}	**1.45 mm**
Uniformity coefficient, c_u	**1.4**
Relative density, D_R	**2.64**
Water content, w	**0.02%**

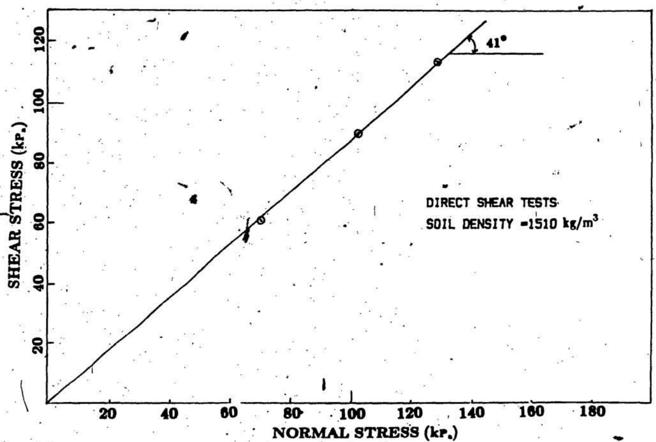

Figure 20: Results of direct shear tests

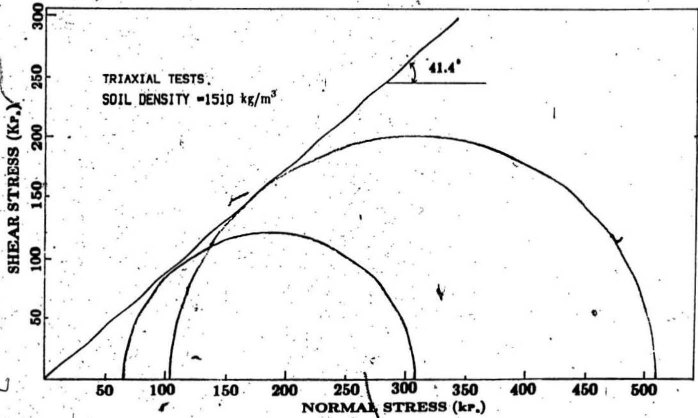

Figure 21: Results of triaxial tests

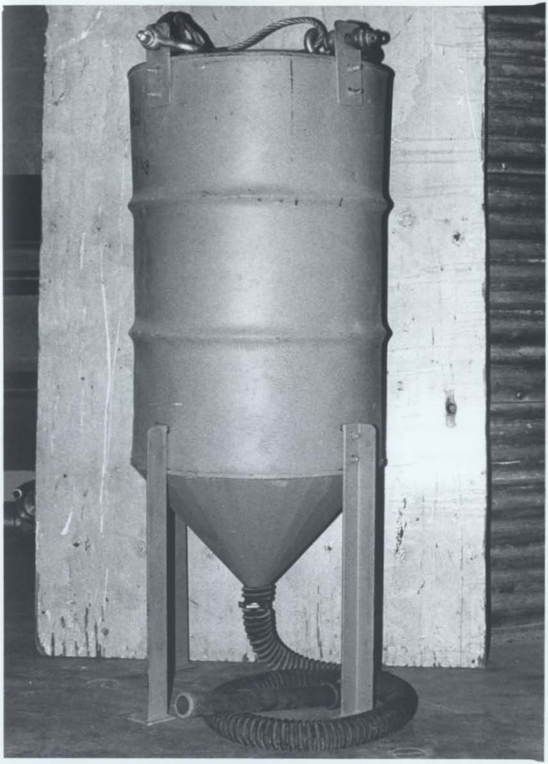

Figure 22: Hopper and hose

3.5 EXPERIMENTAL PROCEDURES

The piles were tested under vertical, lateral and inclined loads. Pull out tests were conducted on vertically loaded piles on completion of the axial tests. The following is the general procedure adopted for all the above tests.

First, the test sand bed was prepared using the raining technique described earlier and the density was checked after each hopper load was poured. If the density was not within the range 1510 $\pm$ 10 kg/m^3, the test was abandoned and a new test bed was prepared.

Secondly, the instrumentation and recording systems were checked using the computer program for the test. The pile and screw jack were mounted and prepared for jacking the pile as shown in figure 9. The pile was lowered to touch the soil and the recording equipment checked manually using the data acquisition unit.

The test pile was then jacked into sand in 50 mm increments using the manually operated screw jack. At each 50 mm increment, the pile penetration was stopped for about 5 seconds to let the soil and equipment stabilize before readings were taken. Then 10 readings were taken for each channel, averaged and recorded on a magnetic disc. Penetration was then continued to the next predetermined depth up to the final depth.

After the final depth of penetration was reached the jack was released. For the axial load tests, at the required depth, the load was applied using the screw jack and the vertical displacements were measured with dial gauges. Pull out tests were then performed on the piles to find the ultimate pull out resistance.

For the horizontal and inclined load tests the 44.5 kN hydraulic screw jack on a swivel joint was installed and set for desired inclination as shown in figure

10. Two LVDT's or dial gauges with a precision of 0.001 mm/div. were mounted and the horizontal deflection and deflection along the load axis were measured as shown in figure 23.

The load was then applied to soil failure or the maximum elastic deflection of the pile material. Data from the load cells, LVDT's and strain gauge bridges were sampled, averaged, and recorded in a manner described earlier. The unloading curve was then established and the data recorded.

The density of the test sand bed was periodically verified using the Fugro-type cone penetrometer. These tests were performed beyond the zone of densification influence around the pile.

At the end of the test, the sand was removed from the soil container by opening the doors on the side of the container.

The results of the tests are presented and discussed in the following chapter along with the various theoretical predictions where such theories are avaiable.

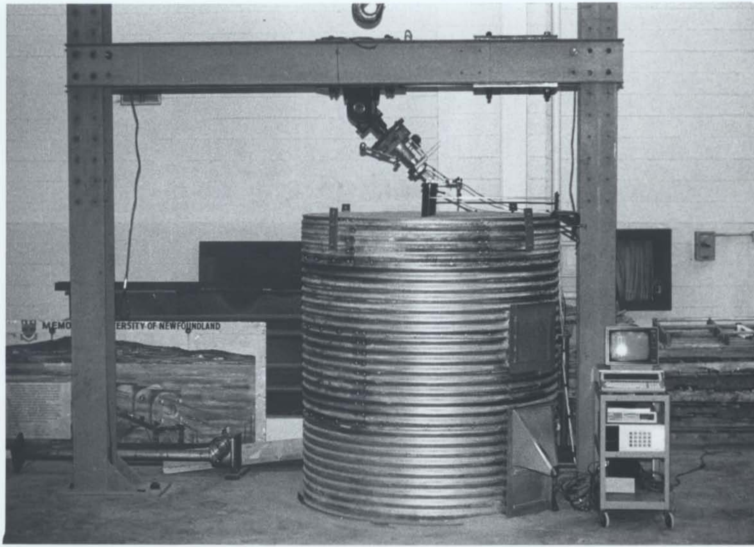

Figure 23: General experimental set up for inclined loads

CHAPTER 4

EXPERIMENTAL RESULTS AND DISCUSSION

4.1 GENERAL

The results of the laboratory tests together with the analysis of the data are presented in detail in this chapter under the following broad categories:

(1) evaluation of the sand bed preparation and uniformity of test conditions as determined by density measurements and cone penetration tests.

(2) Axial loading of piles together with an evaluation of N_q, pile critical depth and determination of pull out resistance.

(3) Lateral loading of piles, ultimate lateral loads and development of p-y curves from the measured bending moment distribution, and comparison with theoretical methods.

(4) Piles under inclined loads and the relationship between the different loading conditions.

4.2 CONE PENETRATION TESTS

In the preparation of the sand bed, the most uniform placement was obtained by raining the sand slowly. After a process of trial and error, a free fall height of 100 mm, and sand laid in layers of 25 mm thickness produced densities of the order 1510 $\pm$ 10 kg/m^3 for all tests and thus it was assumed that the soil bed prepared was consistently uniform.

A further verification of the uniformity of the test bed was made using the electrical cone penetrometer. The variation of static cone pressure with depth for six different tests is shown in Figure 24. It may be observed that the cone pressure increases linearly up to 60 cm and reaches a near critical value. It is also seen that the results of the tests are within ± 5% confirming the uniformity of the sand test bed for the various tests.

The ultimate base resistance for a pile in sand is given as :

$$q_b = \gamma ' D N_q \tag{3}$$

where q_b is the unit base resistance (generally expressed in kPa),

$\gamma '$ is the effective unit weight of soil,

N_q is the bearing capacity factor, and

D is the vertical distance between the ground surface and the pile tip.

The accurate prediction of the base resistance from Equation 3 is complicated by the fact that N_q is not a constant and depends on the angle of internal friction, the ratio of depth to diameter of the pile, and on the relative density of the sand. Experimental results by Kerisel (1964), Vesic (1970), Tavenas (1971) and Meyerhof (1976) indicate that the bearing capacity increases linearly with depth for relatively shallow depths. At a certain critical depth (D_c), which depends on the size of pile and density of sand, the rate of increase of base resistance with depth becomes nonlinear finally reaching a constant or nearly constant value. At shallower depths, the size of the base will influence the unit base resistance, but at greater depths the size appears to have little influence on the value obtained. At depths exceeding 10-20 diameters, the unit base resistance appears to be a function of only the relative density of the sand.

The cone penetrometer results on Figure 24 show that the cone pressure, q_p, tends to become constant below a depth of about 17 times the cone diameter

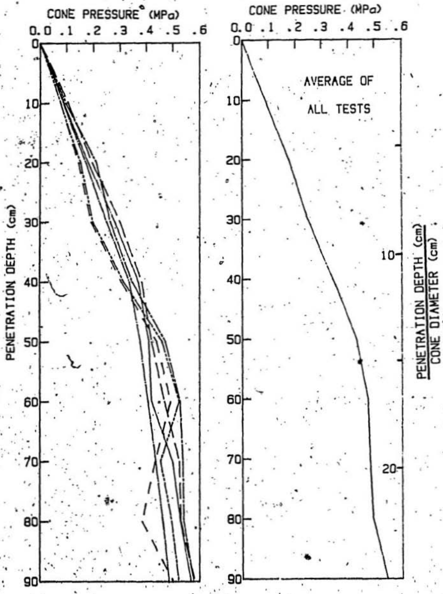

Figure 24: The variation of cone pressure distribution with penetration depth for six typical tests

(17B). This can be taken as the critical depth for the silica sand used in the experiments.

During the cone penetrometer tests the total load on the penetrometer at the top was also measured and the difference between the total load and the cone resistance was taken as the resistance due to skin friction. The total friction as well as the unit frictional stress measured along the length of the penetrometer (expressed as the average skin friction), were computed as shown in Table 5 and Figure 25. It may be seen that there is a reasonably good correlation between the total skin friction computed from sleeve measurement and that obtained from the measured total force on the penetrometer. It may also be seen that the frictional force also approaches a constant value at a depth of about 20 times the diameter.

Cone Penetrometer tests show that the soil bed was uniform and repeatable test conditions were obtained for each test series.

4.3 AXIAL LOAD TESTS ON MODEL PILES

In the first series of tests discussed in this section, the pile was axially loaded to its ultimate bearing capacity and subsequently subjected to pull out tests.

After preparation of the sand bed, the pile was pushed into the sand slowly jacking it at 0.8 mm/s to the predetermined depth. At this depth the load was released and the pile allowed to set.

The total resistance of the pile to penetration was measured by the load cell at the top of the pile, while the end resistance was measured by the load cell at the tip. The difference between the two is the shaft resistance due to skin friction. Typical results of the point resistance as the pile penetrated the sand are illustrated in Figures 26, 27 and 28 for the piles of diameter 25 mm, 42 mm, and 60 mm respectively. The averaged point resistances for the three test piles and also results obtained from the cone penetrometer tests are shown in Figure 29.

From the cone penetrometer tests the critical depth for q_b was found to be about 17 times the cone diameter. It may be seen from Figure 29 that q_b approaches a constant value at a depth to diameter ratio of about 17 to 20 for the three piles. As discussed previously, the critical depth depends on the size of the pile and the relative density of the sand. For the two piles of diameter 25 mm and 42 mm which were pushed to D/B ratios of over 30, the critical depth can be identified. For the pile of diameter 60 mm which has reached a maximum D/B ratio of about 25 the critical depth is not yet well defined.

The above results confirm the behavior of piles under axial loads and verify the concept of critical depth which has been proposed by various researchers.

4.3.1 LOAD TESTS - LOAD/SETTLEMENT CURVES

After the piles were pushed to the required depth, load tests were conducted and the load-settlement curves were obtained as shown in Figure 30. The loading procedure and a description of the equipment and instrumentation were described in Chapter 3. While the 25 mm and 42 mm piles were tested at a D/B ratio of 40 and 31 respectively, the 60 mm diameter pile was tested at three different D/B ratios as shown in Figure 31.

The ultimate or failure load condition can be interpreted in several different ways from a load-settlement curve. The criterion for establishing the ultimate load from load-settlement curves has been discussed by Whitaker (1963), Vesic (1967), Tomlinson (1977), and Poulos and Davis (1980). The point on the load settlement curve where the curve becomes straight or substantially straight is generally taken as the failure load and these are so identified in Figures 30

Table 5

The average results of six cone penetrometer results given in Figure 24

DEPTH (mm)	Q_T (N)	Q_P (N)	Q_T-Q_P=Q_s (N)	q_p (kPa)	q_s (kPa)
200	184	175	8	175	.7
300	262	247	12	247	.72
400	565	342	21	342	.94
500	469	430	35	430	1.24
600	518	473	42	473	1.26
700	534	482	52	482	1.3
800	543	492	51	492	1.12
900	599	541	58	541	1.14

$q_p = Q_P/A_S$

$Q_s = Q_S/(0.5\text{x}A_S)$ at a given depth above critical depth

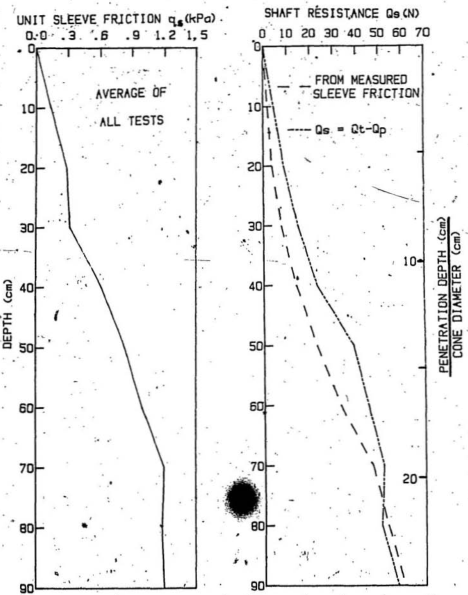

Figure 25: The averaged variation of unit sleeve friction and shaft resistance with penetration depth

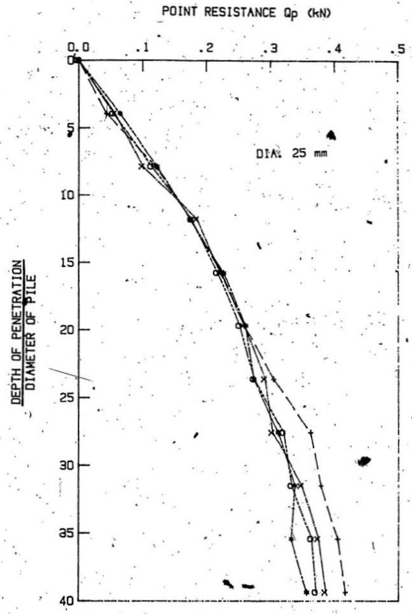

Figure 26: The variation of point resistance with relative depth for 25 mm diameter pile .

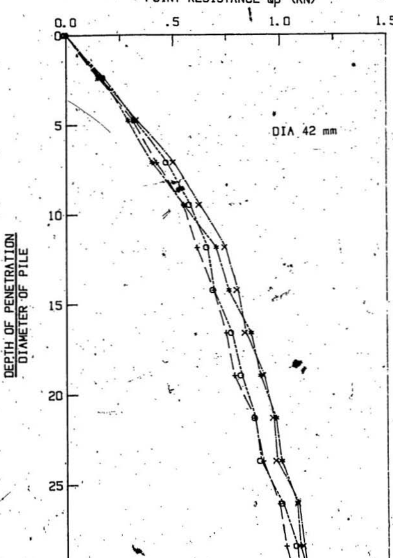

Figure 27: The variation of point resistance with relative depth for 42 mm diameter pile

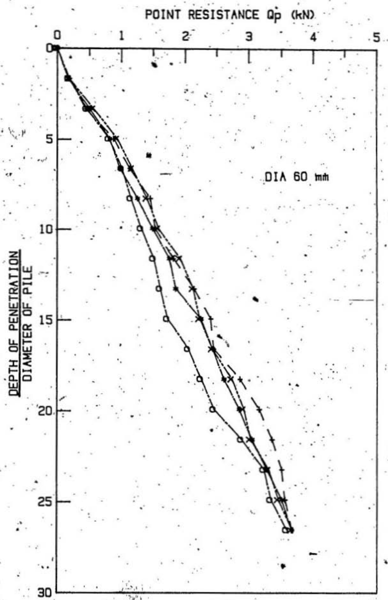

Figure 28: The variation of point resistance with relative depth for 60 mm diameter pile

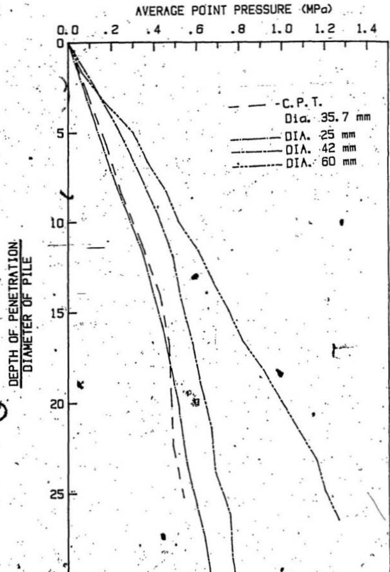

Figure 29: A comparison of average point pressure for model piles and cone penetrometer with relative depth

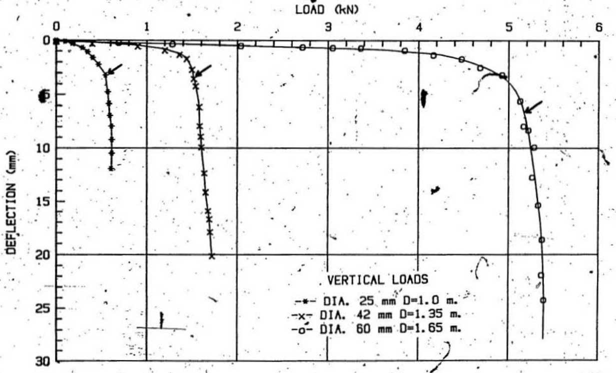

Figure 30: The load-settlement curves for model piles under vertical loads

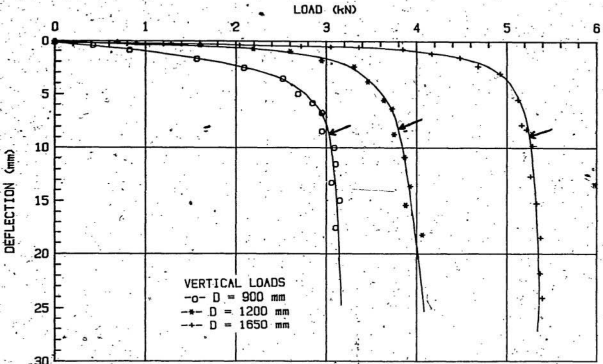

Figure 31: The load-settlement curves for a 60 mm diameter pile under vertical loads

and 31. It is, however to be noted that some degree of subjectivity is involved in identifying the failure load and consistent and reliable interpretation of test results requires some familiarity, experience, and judgement.

A number of theoretical and empirical expressions for determining the bearing capacity factors were discussed in Chapter 2. While verifying the experimental results, comparisons were made using the theories of Terzaghi (1943), Brinch Hansen (1951), Berezantzev (1961), Durgonoglu and Mitchell (1973), Meyerhof (1976), Vesic (1977) and Fleming et al (1985) to compute the end bearing resistance. The theoretical and experimental results are tabulated in Table 6 and also compared in Figures 32, 33 and 34 for all three piles.

Theoretical and measured values of N_q are compared in Figure 35. It is seen that the experimental values are closest to the theoretical values of Vesic (1977). It may also be seen that the values of q_b calculated by the iterative procedure proposed by Fleming et al (1985) approaches a constant value with increasing depth. This limiting behaviour was earlier attributed to some form of arching effect. Fleming et al (1985) explain that a more rational explanation lies in the variation of friction angle, ϕ', with confining pressure. This approach in computing the critical depth is different from those suggested by other authors based on the pile D/B ratio.

Kerisel (1964) and Meyerhof (1976) reported that the value of N_q in sand increases with depth and reaches its maximum value at less than half the critical depth while Berezantzev (1961) indicated a decrease of N_q with depth. Drugunoglu and Mitchell (1973) found that N_q increases with increasing D/B ratio, while Vesic (1977) concluded that N_q is a constant independent of depth. The variation of N_q obtained from present tests (Figure 35) show an agreement with the conclusions of Berezantzev (1961) that there is in fact a slight decrease in N_q

Methods	PILE DIAMETER											
	25 (mm)				42 (mm)				60 (mm)			
	D	Q_p	Q_s	Q_u	D	Q_p	Q_s	Q_u	D	Q_p	Q_s	Q_u
Terzaghi (1943)	1000	0.93	0.24	1.17	1350	3.15	0.67	3.82	900 1200 1650	4.45 5.93 8.15	0.46 0.57 1.52	4.91 6.5 9.67
Berezantzev (1961)	1000	1.35	.24	1.59	1350	4.59	0.67	5.26	900 1200 1650	6.48 8.64 11.89	0.46 0.57 1.52	6.94 9.21 13.41
Mitchell (1973)	1000	0.75	0.24	0.99	1350	2.53	0.67	3.20	900 1200 1650	3.58 4.77 6.57	0.46 0.57 1.52	4.04 5.34 8.09
Meyerhof (1976)	1000	2.75	0.24	2.99	1350	9.34	0.67	10.0	900 1200 1650	13.2 17.6 24.2	0.46 0.57 1.52	13.65 18.16 25.7
Vesic (1977)	1000	0.63	0.24	0.87	1350	2.13	0.67	2.80	900 1200 1650	3.01 4.02 5.53	0.46 0.57 1.52	3.47 4.59 7.05
Fleming (1985)	1000	0.98	0.24	1.22	1350	3.09	0.67	3.76	900 1200 1650	5.03 5.94 7.39	0.46 0.57 1.52	5.49 6.51 8.91
B.Hansen (1951)	1000	1.61	0.24	1.85	1350	5.47	0.67	6.14	900 1200 1650	7.73 10.3 14.2	0.46 0.57 1.52	8.19 10.9 15.7
Experiment	1000	0.48	0.12	0.60	1350	1.29	0.28	1.57	900 1200 1650	2.54 3.22 4.45	0.53 0.62 0.81	3.07 3.84 5.26

Table 6

Comparison of theoretical and measured ultimate bearing loads (kN)

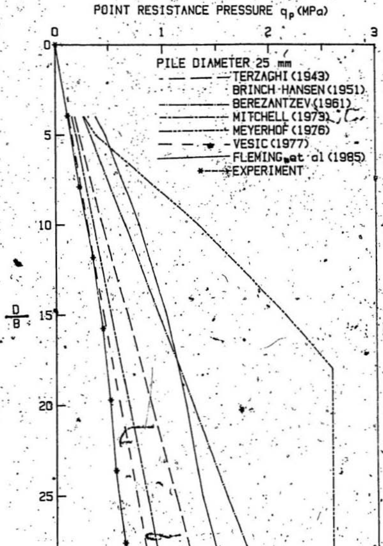

Figure 32: A comparison of theoretical and experimental point resistance pressures with relative depth for a 25 mm diameter pile

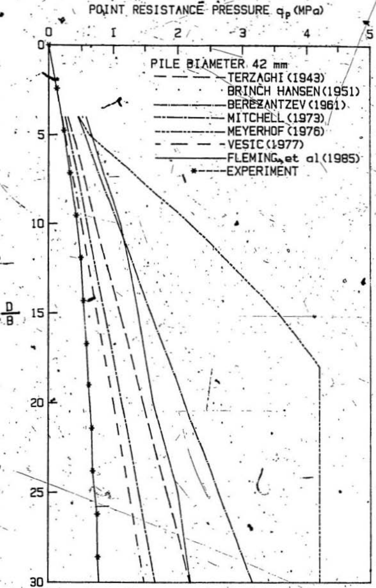

Figure 33: A comparison of theoretical and experimental point resistance pressures with relative depth for a 42 mm diameter pile

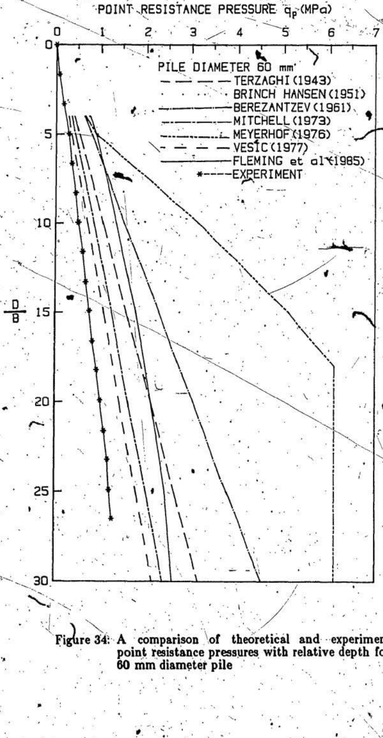

Figure 34: A comparison of theoretical and experimental point resistance pressures with relative depth for a 60 mm diameter pile

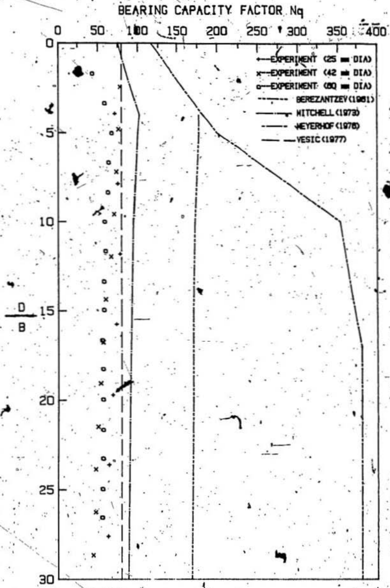

Figure 35: The variation of bearing capacity factor N_q with relative depth

with depth.

4.3.2 SKIN FRICTION

Piles usually receive support from both end-bearing and shaft resistance. The relative magnitude of the shaft and base capacities will depend on the geometry of the pile and the soil profile. The averaged values of the point and shaft resistance, during pile penetration, are shown in Table 7 and Figure 36. Shaft friction is in the order of 5-15% of the total ultimate resistance and can be considered as negligible for normal practice of designing piles in cohesionless soils.

The unit frictional resistance q_s, in sand at a depth z, is given by

$$q_s = K_s \, \sigma' \tan \delta \tag{9}$$

where K_s denotes the coefficient of earth pressure on the pile shaft,

σ' is the average effective overburden pressure, and

δ is the angle of friction between the soil and pile material.

Equation 9 can be rewritten integrating along the embedded pile length D, for the total shaft resistance Q_s, as follows:

$$Q_s = 0.5 \, K_s \, \gamma' D \tan \delta \, A_s \tag{10}$$

where A_s is the total area of the embedded pile shaft.

Factors K_s and $\tan \delta$ need to be established in order to determine unit skin resistance. The most sensitive and elusive factor is K_s, which depends on the method of installation of the pile and the initial density of sand. Coyle and Castello (1979) concluded that the value of K_s is not uniform and varies with depth from the passive to the active pressure range.

Table 7

Values of measured point resistance force and shaft resistance

Depth (cm)	Pile diameter								
	25 mm			42 mm			60 mm		
	Q_T	Q_b	Q_s	Q_T	Q_b	Q_s	Q_T	Q_b	Q_s
20	143	114	29	336	316	20	594	490	104
30	214	177	37	475	451	24	995	854	141
40	266	222	44	619	578	41	1238	1066	172
50	323	258	65	732	681	51	1544	1312	232
60	354	286	68	807	737	70	1723	1474	249
70	391	324	71	896	808	88	2063	1745	318
80	414	349	76	965	859	106	2268	1930	338
90	431	368	87	1027	927	102	2604	2150	454
100	454	382	119	1111	952	159	2858	2340	518
110				1236	1053	184	3138	2614	524
120				1324	1070	254	3426	2843	583
130				1376	1109	267	3704	3076	628
140							3767	3325	642
150							4148	3459	689
160							4384	3637	747

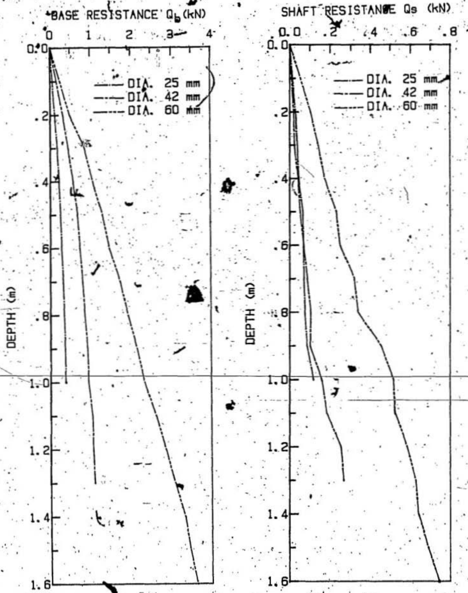

Figure 36: The variation of point resistance and shaft resistance with depth

From the model pile tests reported here, a trend has been observed for skin friction similar to that for end-bearing pressure (Vesic, 1977). The shaft friction tends towards some limiting value with increasing depth. Cone penetrometer tests (Figure 25) confirm the phenomenon. The possibility of a critical depth for skin friction may be a topic of further research.

4.3.3 PULL OUT RESISTANCE

Piles are generally used to support compressive loads from superstructures. Some structures, like transmission towers, mooring systems for submerged platforms, tall chimneys, jetty structures, etc., are constructed on pile foundations, and are subjected to uplift forces. The behaviour of piles subjected to such uplift loads have not been fully understood as yet. Moreover, there are differing views about push-in and pull-out shaft friction.

Broms (1963), Mohan et al (1963), Hunter and Davisson (1969), and Sowa (1970) have shown that pull-out shaft friction is significantly less than push-in friction. Poulos and Davis (1980) suggest evaluating the uplift capacity of a vertical pile by reducing to 2/3, the calculated shaft resistance for downward loading. On the other hand Ireland (1957), Vesic (1970) and Ismael and Klym (1979) suggest that there is no significant difference between the two.

Fleming et al (1985) state that there is no systematic difference in the value of skin friction which may be mobilized by a pile loaded either in tension or compression, except for relatively slender piles. They attribute the discrepancy in the pull out and push-in values to residual stresses which exist after pile installation leading to an under-estimation of the end-bearing capacity of the pile, thus overestimating the skin friction in compression. In most experimental studies uplift loading is applied after the pile had first been tested to failure in compression which was the case in this experimental study. Pull out tests were conducted on the piles and load-deflection curves obtained as shown in Figure 37.

A number of theories have been put forth to compute the pull out resistance of piles in sand Meyerhof (1973), Poulos (1980), Levacher and Sieffert (1984), and Chattopadhyay and Pise (1986). Table 8 shows the computed pull out resistance, measured shaft friction and measured pull out resistance. It is seen that there is considerable variation between the measured and computed values. The measured values are similar to those obtained by Chaudhuri and Symons (1983), who concluded that theoretical predictions are in significant error when compared with experimental results. It may be seen from Table 8 that the skin friction in tension is about 75% of the shaft resistance in compression.

4.4 VERTICAL PILE UNDER LATERAL LOADS

The second series of tests consisted of a vertical pile subjected to horizontal loads at the top of the pile. The piles were instrumented with electrical resistance strain gauges, details of which were described in Chapter 3. The gauges were used to obtain the bending moment in the piles along their length. The results of the lateral load tests and derivation of p-y curves from the resulting bending moment diagrams are discussed in this section.

4.4.1 MEASURED LOAD VERSUS DEFLECTION

The horizontal deflection at the top of the pile was measured by gradually increasing the lateral loads. Load deflection curves were obtained and the unloading behaviour of the pile investigated on completion of the test. Typical load-deflection curves for the top of the pile for piles of 25 mm, 42 mm, and 60 mm diameters are shown in figure 38. In all these tests the pile behaved as a long flexible pile and it was ensured that the bending stresses in the pile shaft

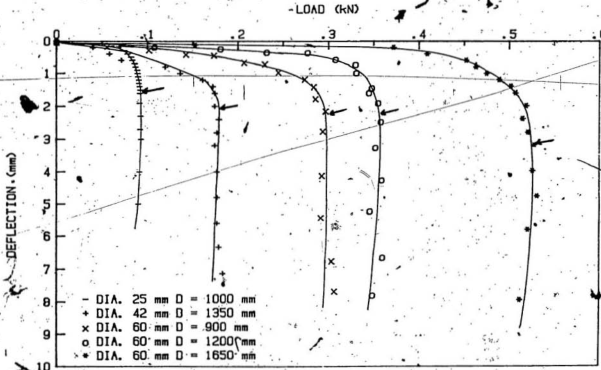

Figure 37: Load test curves for piles subjected to pull out forces

Table 8

Pull out resistance (kN)

Pile Dia.	D/B	Q_s	W	Theory 1	2	3	4	Experiment Q_u - Q_b	Meas.
25 mm	40	0.24	0.04	0.20	1.73	0.17	0.26	0.12	0.09
42 mm	32	0.71	0.08	0.56	5.18	0.50	1.0	0.28	0.18
60 mm	15	0.45	0.14	0.44	3.40	0.32	1.37	0.53	0.30
60 mm	20	0.81	0.14	0.68	5.93	0.57	1.83	0.62	0.36
60 mm	27	1.53	0.14	1.16	11.08	1.07	2.51	0.81	0.53

$Q_s = 0.5K\,\gamma\tan\delta A_s$

(1) Poulos [$(2/3)Q_s$ + W]

(2) Meyerhof [$B\gamma D^2 K_b/2$ + W] (for rough piles)

(3) Levacher [$0.5K_o\,\gamma PfH^2K_{mo}$

(4) Chattopadhyay

W -weight of pile

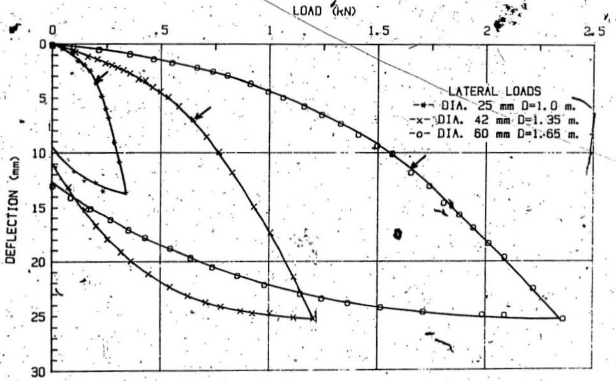

Figure 38: Load-deflection curves for model piles under lateral loads

were in the elastic range.

It may be seen from the load-deflection curves that the deflection at the top of the pile is a nonlinear function of load. The unloading behaviour of the pile confirms this and there is a permanent deformation of the soil.

4.4.2 MEASURED BENDING MOMENT DISTRIBUTION

During the lateral load tests the strain gauges were used to continuously monitor the bending strains at various points along the length of the pile shaft. The output voltage for each bridge at each load level multiplied by its calibration constant (Figure 18) gave the bending moment in the pile at that level for that load step.

The measured bending moment for piles of diameters 25 mm, 42 mm, and 60 mm are illustrated in Figures 39, 40, and 41. For clarity, curves are only shown for five load cases; loads were applied and similar curves obtained for various load increments. One characteristic of the curves that was observed was that the point of maximum moment moves downward as the load increases. Also, near the point of maximum moment, the curvature increases with increasing lateral load.

p-y curves were developed using the bending moment distribution curves and the pile head deflections. These curves were compared with curves derived from different theoretical methods and discussed in a subsequent section.

4.4.3 DEVELOPMENT OF p-y CURVES

When a lateral load is applied to the top of a flexible pile, the load is transferred to the soil surrounding the pile. Before any lateral load is applied to the pile the resultant force obtained by integrating the pressure around the pile

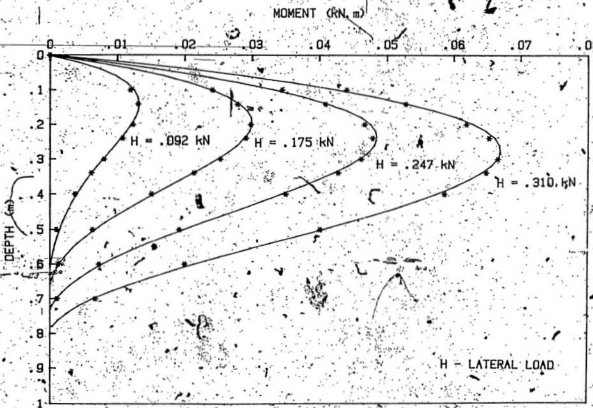

Figure 30: Bending moment distribution curves for 25mm diameter pile.

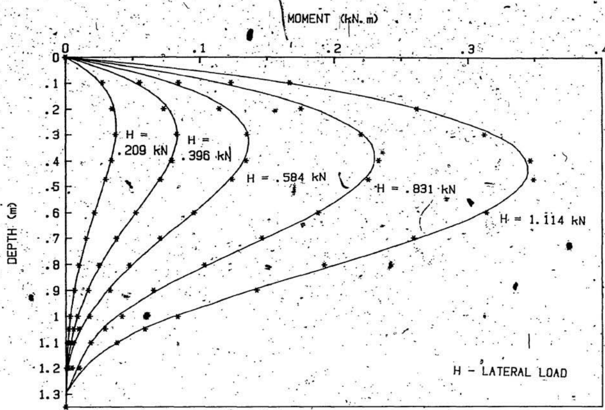

Figure 40: Bending moment distribution curves for 42 mm diameter pile

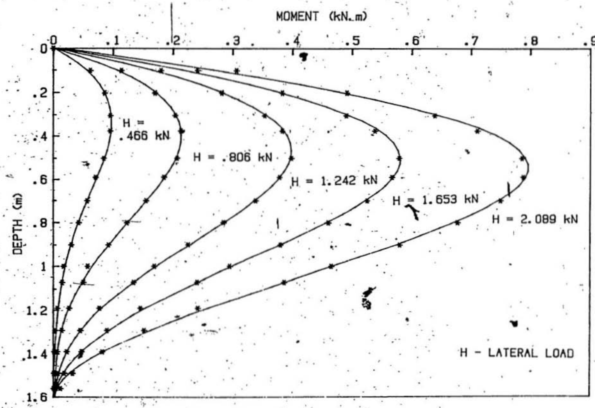

Figure 41: Bending moment distribution curves for 60 mm diameter pile

will be zero (Figure 4). The deflection y, of a pile due to an applied load generates an unbalanced force p, per unit length of pile. This unbalanced force per unit length is unique at each point along the length of the pile and is a function of the pile deflection at that point. Thus, for a series of deflections, the corresponding series of forces may be combined to obtain a p-y curve corresponding to a given depth. The maximum possible pressure that can be developed in the sand is equal to the passive resistance of the sand. p-y curves are generally used as a technique for introducing effects of material non-linearity and non-homogeneity into the elastic subgrade reaction model for the soil.

Various methods of determining the p-y curves have been proposed in the literature by Matlock and Ripperger (1956), Reese et al (1969), Reese et al (1974) and Reese et al (1975). The method for obtaining the best correlation is to determine the experimental p-y curves with a simultaneous measurement of bending moment distribution in the pile.

For a given value of applied load and moment at the pile head, the measured distribution of bending moment M, along the pile length can be used to obtain the corresponding distribution of pile displacement y, and the soil reaction p.

The deflection can be obtained by successive integration as :

$$\iint \frac{M}{EI}\, dx \qquad (27)$$

The soil reaction (load distribution) can be obtained by successive differentiation as :

$$p = \frac{d^2M}{dx^2} \qquad (28)$$

Appropriate boundary conditions must be used, and the equations solved numerically as discussed in the next section.

A series of p-y curves corresponding to various depths in the soil may be generated by plotting corresponding values of p and y at each depth for increasing levels of lateral loading.

4.4.4 CURVE FITTING PROCEDURE

In the analysis of the test data to obtain deflection, slope, moment, shear and soil reaction curves, the data can be properly fitted finding a continuous mathematical function that would adequately describe the variation of moment with depth. This function could be a truncated power series, trigonometric series or a spline function. An alternative procedure would be to fit a function over a selected interval and then operate on the function within the interval, successively changing the interval until all data points had been operated upon. The most convenient function to use (Welch 1972, Pise 1977), from the standpoint of simple differentiation and integration is a polynomial describing a truncated power series.

A polynomial describing a truncated power series was adopted in this thesis in fitting a function to the measured bending moment distribution. A least-squares curve fitting technique was used to fit the polynomial to the data. In fitting a polynomial to the data, the question of the degree of polynomial to use has to be determined. The polynomial would have to be in the order of three or greater, since soil reaction is determined by differentiating twice. Also the greater the degree of the polynomial the better would be the curve fit, but with a greater possibility of erratic behaviour between points. Polynomials of degree four through ten were fitted to the moment curves and the first derivative compared to the applied shear (lateral load). The second derivative was examined for its sensitivity with the change in the degree of the polynomial. It was concluded that the polynomial of degree-seven would provide the best curve-fit without erratic behaviour.

The deflection of the pile along its length was determined by integrating the fitted moment curve twice using Simpson's rule. It was found that the two independent boundary conditions, the measured deflection at the top of the pile and an assumed zero deflection at the bottom of the pile yielded similar deflection curves along the length of the pile . The shear resisted by the pile was determined by differentiating the fitted curve. The second derivative yielded values of soil reaction. A computer program was written for the least-squares curve fitting procedure, the numerical integration using Simpson's rule and differentiation using finite difference methods (Appendix A). A typical solution showing the deflection, slope, moment, shear and soil reaction as a function of depth is presented in Figure 42.

4.4.5 p-y CURVES

From the experimental moment curves measured during the lateral load tests, values of the soil reaction p, and deflection y, were obtained using the numerical procedure described above. Typical p-y curves for pile diameters of 25 mm, 42 mm and 60 mm are shown in Figures 43, 44 and 45.

It may be seen from these curves that there is evidence of initial elastic behaviour of the soil and the elastic range is generally associated with smaller displacements. Also, for similar soil displacement, the soil reaction increases with increasing depth of the soil. Thus, the initial slope of the p-y curve increases with depth. The curves tend to become horizontal, indicating that the ultimate

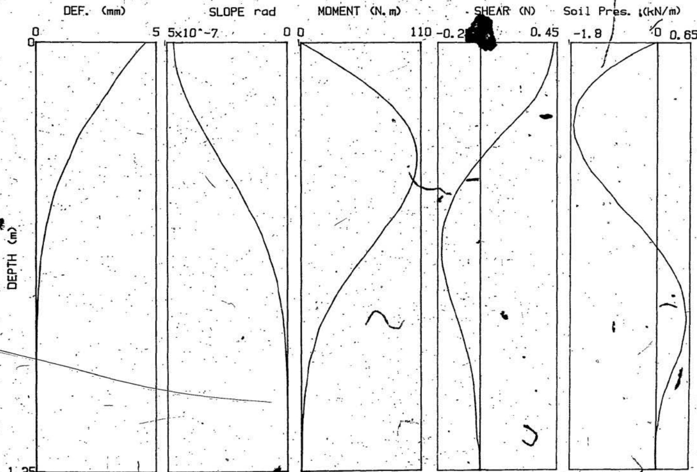

Figure 42: Complete solution of laterally loaded pile

resistance of the sand is achieved or is approaching.

Curves are shown for depths up to five pile diameters only, since for larger depths the pile displacements and soil reactions are too small for accurate determination of the p-y relationship. Barton et al (1983) state that distributions of soil reaction p, derived from experimental data require careful interpretation and are best regarded as indications of the general variation in the soil reaction rather than exact values. Another limiting factor is that the ultimate soil reaction is only developed up to a depth of about five pile diameters because the application of larger loads would have stressed the steel beyond the linear stress range.

To check the accuracy of the experimentally derived p-y curves, the lateral load-pile head deflections and moment curves were computed using the computer program developed by Reese and Monoliu (1973) and extended by Reese (1975b, 1977). The differential equation (equation 25) described in Chapter 2 is solved using successive difference equations based on repeated reference to the p-y curves. The computed and experimental load-deflection curves are shown in Figure 46. The corresponding bending moment distribution curves are shown in Figures 49, 50, and 51, for the piles of diameter 25 mm, 42 mm and 60 mm respectively. There is good agreement between the computed and experimental values and the p-y curves derived from the experimental data are consistent with those suggested in the published literature.

4.4.6 ULTIMATE LATERAL SOIL RESISTANCE

Reese et al (1974) suggest two modes of failure when a pile moves laterally through the soil. Near the ground surface the resistance is controlled by a passive failure wedge. For greater depths the resistance is assumed to be primarily by flow of sand around the pile. The expressions (Equations 18 and 19) are used

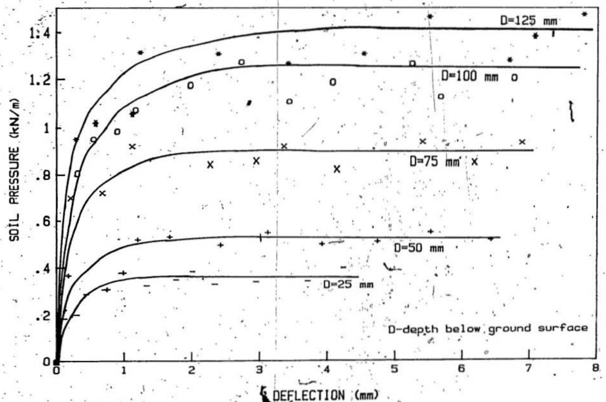

Figure 43: p-y curves for 25 mm diameter pile

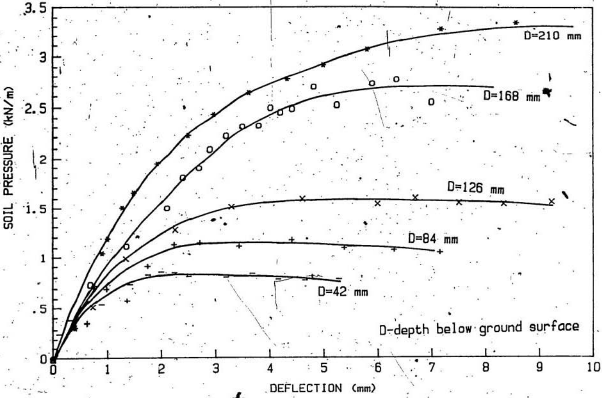

Figure 44: p-y curves for 42 mm diameter pile

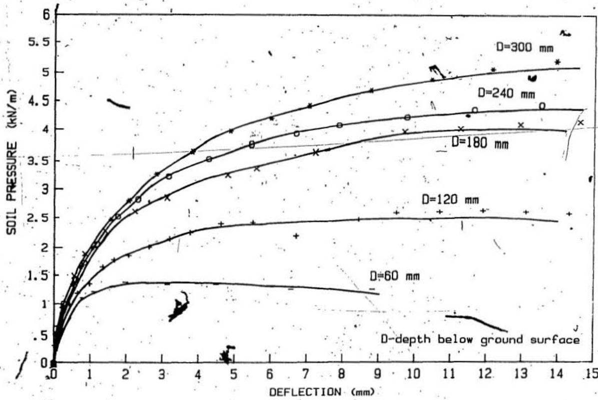

Figure 45: p-y curves for 60 mm diameter pile

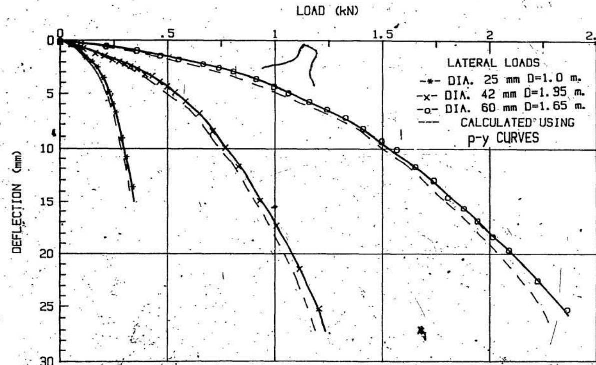

Figure 46: Load-deflection curves for model piles under lateral loads

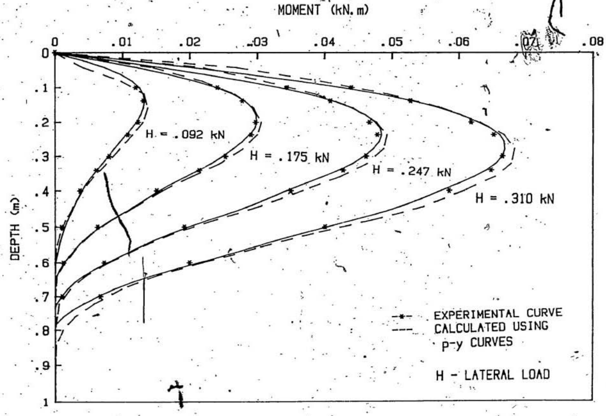

Figure 47: Bending moment distribution for 25 mm diameter pile

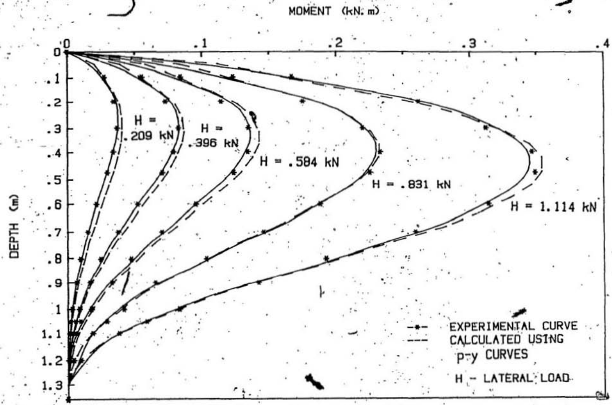

Figure 48: Bending moment distribution for 42 mm diameter pile

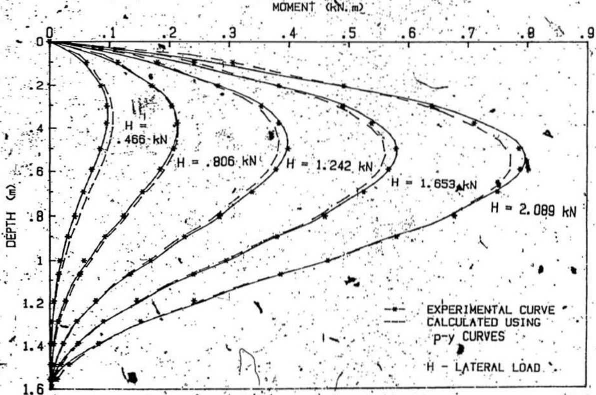

Figure 49: Bending moment distribution for 60 mm diameter pile

for computing the ultimate soil resistance and the smaller of the two values adopted.

Broms (1964) has suggested a net limiting force per unit length of pile ,p_u given by

$$p_u = 3\,K_p\,\sigma_v\,'D \qquad (29)$$

Broms has prepared charts in non-dimensional form giving the lateral capacity of piles in terms of plastic moment and geometry of piles.

An intermediate variation of limiting pressure with depth is to take p_u proportional to the square of the passive earth pressure coefficient ,K_p, giving

$$p_u = K_p^{\,2}\sigma_v\,'D \qquad (30)$$

Figures 50, 51, and 52 show the calculated values of average limiting force per unit length with depth, compared with the three methods discussed above. It may be seen that Broms (1964) method underestimates the limiting pressure except very close to the ground surface. The limiting pressures closely follow the variation given by Reese et al (1974) and that computed by Equation 29. At depths greater than five pile diameters it may be noted that both the methods overestimate the ultimate soil pressure. Hence, it is recommended that the the ultimate soil pressure at a depth of five pile diameters be adopted as the limiting value for greater depths.

4.4.7 MEASURED AND PREDICTED LATERAL PILE RESPONSE

The moment distributions and deflected shapes under applied lateral loads for the piles of diameter 25 mm, 42 mm and 60mm were computed and compared with the measured values. In the computation of the pile behaviour the soil

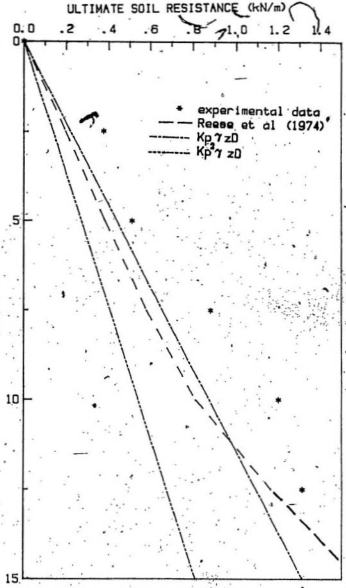

Figure 50: Ultimate soil resistance vs. depth for 25 mm diameter pile

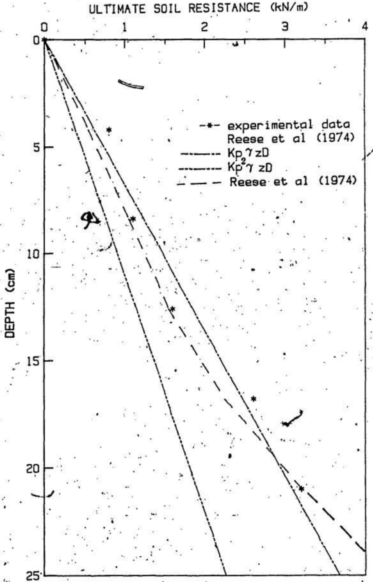

Figure 51: Ultimate soil resistance vs. depth for 42 mm diameter pile

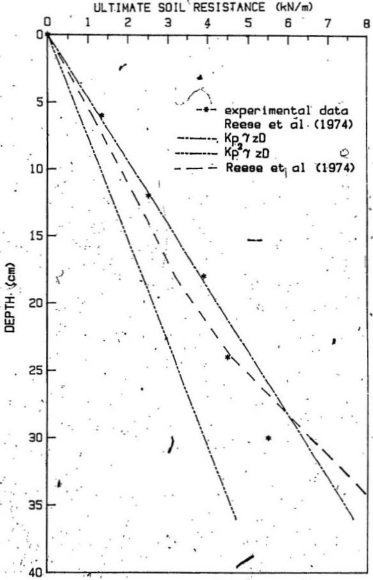

Figure 52: Ultimate soil resistance vs. depth for 60 mm diameter pile

response was predicted by the semi-empirical methods of Reese et al (1974), Matlock et al (1980), Scott (1980) and Parker (1974). The pile response was computed using the program developed by Reese (1977) as described earlier.

Measured and predicted bending moment distributions for piles of diameter 25 mm, 42 mm and 60 mm are illustrated in Figures 53, 54, and 55 for five typical load cases. It may be seen that at small loads all the methods show good agreement with the measured values and follow the general trend of the measured moment curves.

Scott's (1980) method underestimates the moments at higher loads and does not agree with the measured values. Parker's (1970) method overestimates the moment values but follows the general pattern of the measured values. Reese et al (1974) and Matlock et al's (1980) methods show good agreement with the overall results but underestimates the moment values for the 60 mm pile, while overestimating the moment values for the 25 mm and 42 mm diameter piles.

For practical problems, the most important aspect illustrated by the comparison is the close agreement obtained for the magnitude and location of the maximum moment. The magnitude and location of the maximum moment will be of primary importance for design problems.

Measured and predicted deflected shapes are shown in Figures 56, 57, and 58 for the 25 mm, 42 mm and 60 mm diameter piles. The predicted deflected shapes were obtained by double integration of the moment curves as described earlier. Curves obtained by the methods of Reese et al (1974) and Matlock et al (1980) show good agreement with the measured values throughout the deflected shape. Parker's (1980) method overestimates the deflections, but follows the general trend of the experimental curves. Scott's (1980) method underestimates the deflections by more than 100%. It may also be noted that the curves obtained

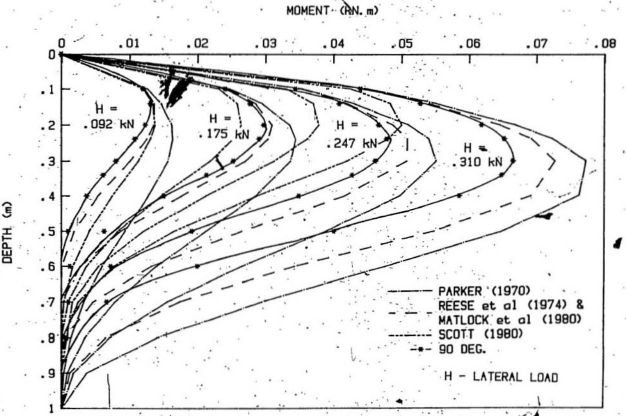

Figure 53: Bending moment distribution curves for 25 mm diameter pile

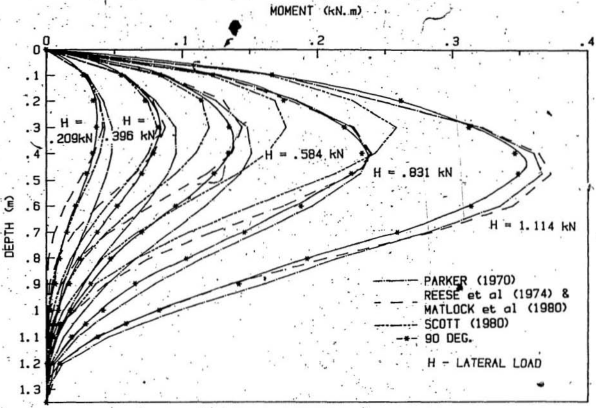

Figure 54: Bending moment distribution curves for 42 mm diameter pile

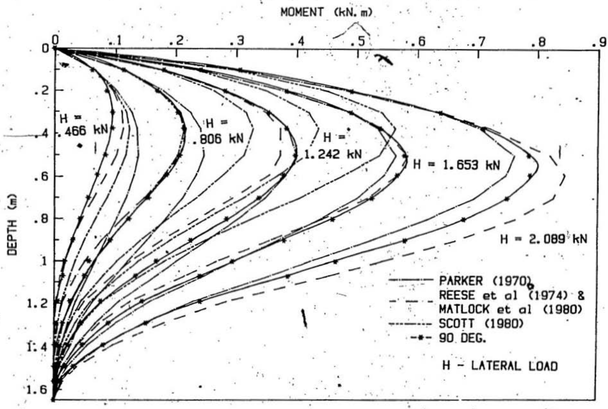

Figure 55: Bending moment distribution curves for 60 mm diameter pile

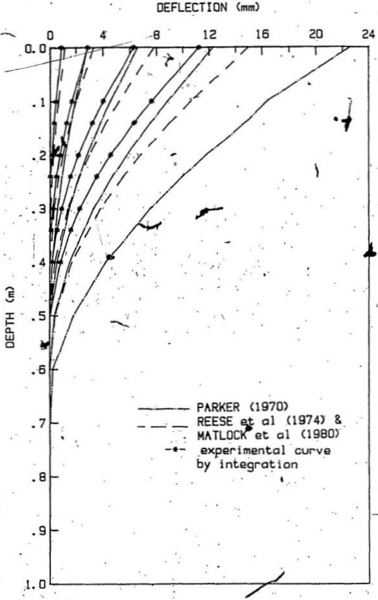

Figure 56: Deflected shapes for 25 mm diameter pile

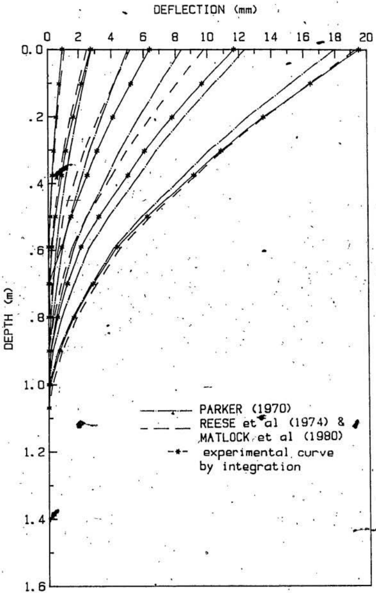

Figure 57: Deflected shapes for 42 mm diameter pile

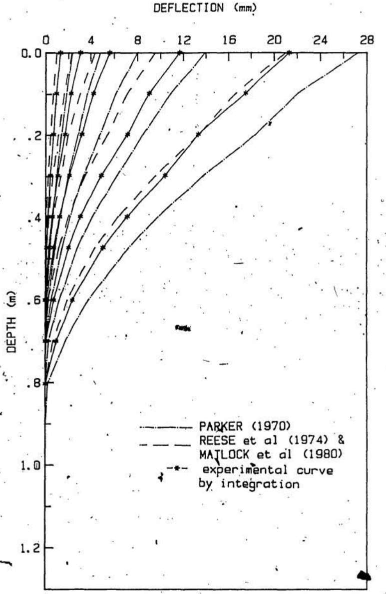

Figure 58: Deflected shapes for 60 mm diameter pile

by the empirical methods have the points of zero deflection deeper than those obtained experimentally.

From the standpoint of understanding the behaviour of the piles and for practical problems the behaviour of the top of the piles is of primary importance. Therefore, the most important aspect illustrated by the comparisons is the relatively good agreement between the measured and predicted deformations in the upper portion of the pile.

4.5 VERTICAL PILE UNDER INCLINED LOADS

The behaviour of vertical piles under inclined loads was studied in the final series of tests. Available data on the behaviour of flexible piles subjected to inclined loads are scarce. The effect of vertical load on the flexural behaviour of piles is not usually considered. Ramasamy et al (1982), however state that that the lateral deflection at the head of a free standing pile can be large and this may result in the vertical load causing an additional moment which tends to magnify the lateral deflection. The behaviour of a pile subjected to inclined loads was investigated and compared with that of a pile acted upon by only lateral loads.

The sand bed was prepared similar to the other tests and the pile was jacked slowly into the sand as described earlier. The swivel joint was used to set the desired angle of inclination and loads were applied by using the 44.5 kN hydraulic jack (Figure 10). The load on the pile, the bending strains, inclined and lateral deflections were measured as described earlier for the lateral load tests, and recorded using the data acquisition system.

Typical load deflection curves for the top of the pile for piles of 25 mm, 42 mm, and 60 mm diameters are shown in Figures 59, 60 and 61. The ultimate inclined load was identified for each curve in a similar manner to that described

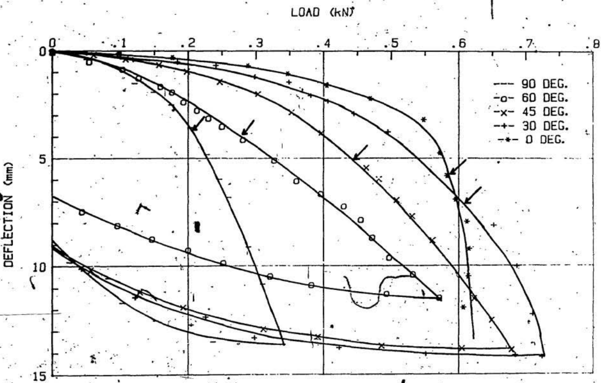

Figure 59: Load-deflection curves for 25 mm diameter pile under inclined loads

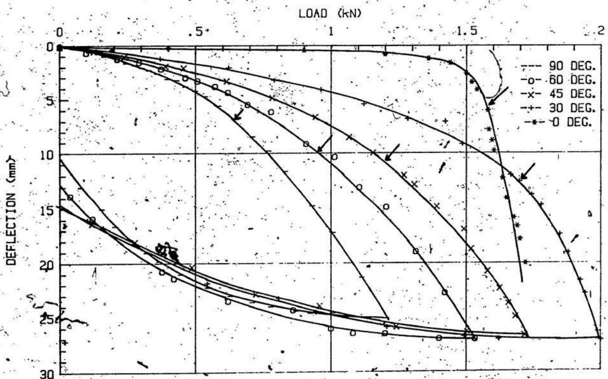

Figure 60: Load-deflection curves for 42 mm diameter pile under inclined loads

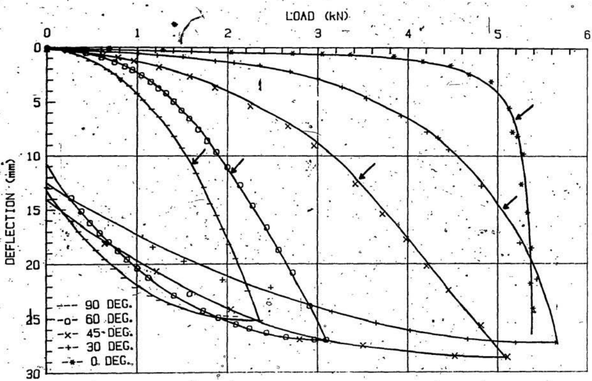

Figure 61: Load-deflection curves for 60 mm diameter pile under inclined loads

earlier for lateral load test results. It may be seen that the load-deflection curves are similar to the lateral load-deflection curves and that the deflection at the top of the pile is a nonlinear function of load.

The ultimate pile capacity under inclined loads was also computed as a percentage of the ultimate vertical load capacity for different values of α. The results are shown in Figure 62. It is seen that the inclination of the load reduces the ultimate capacity of the pile with a rapid reduction for load inclinations between 45 and 60 degrees. These experimental results are similar to those reported by Meyerhof and Ranjan (1972) and Chari and Meyerhof (1983) for rigid piles in sand.

4.5.1 MEASURED AND THEORETICAL p-y CURVES

Values of soil resistance p, and deflection y, were obtained from the measured bending moment distribution curves for the inclined load tests in a manner similar to that discussed earlier for the lateral load tests. Theoretical p-y curves proposed by Reese et al (1974), Matlock et al (1980), Scott (1980) and Parker (1970) were also computed and plotted together with the experimental curves as shown in Figures 63 through 77. The experimental data was best fitted by drawing a smooth curve. It may be noted that there is no difference in the p-y curves for the methods of Reese et al (1974) and Matlock et al (1980), since the second procedure is a simplification of Reese et al's (1974) method.

The experimental curves follow the same general trends as the curves of Reese et al (1974), Matlock et al (1980) and Parker (1970). There is an initial elastic range and the curves become horizontal when the ultimate resistance of the soil is achieved. Scott's (1980) results differ from the experimental values as his method assumes an unlimited linear increase in soil resistance with increasing

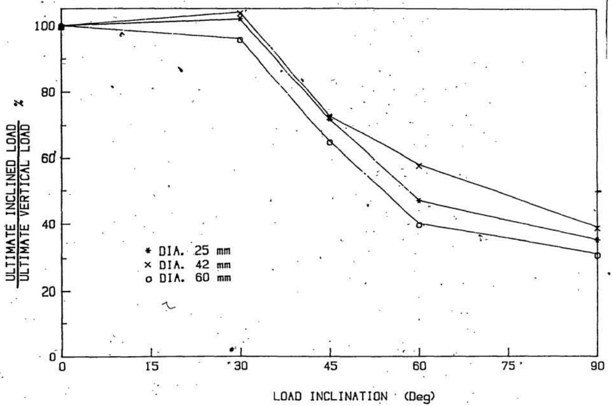

Figure 62: Effect of load inclination on ultimate pile capacity

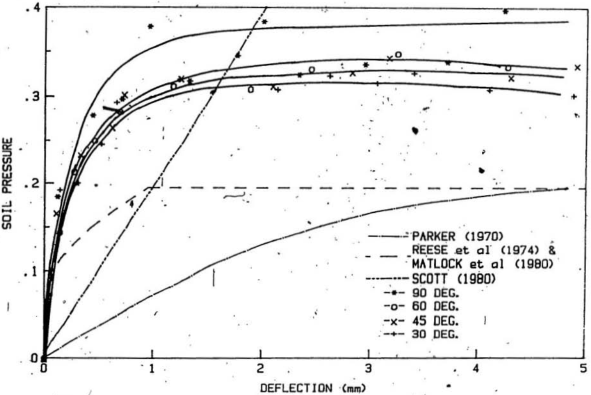

Figure 63: p-y curves for 25 mm diameter pile at depth 25 mm

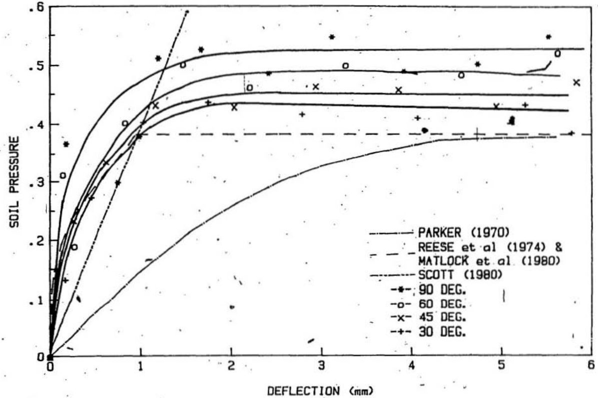

Figure 64: p-y curves for 25 mm diameter pile at depth 50 mm

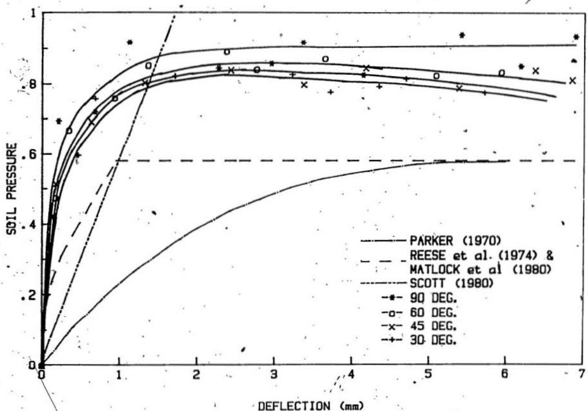

Figure 65: p-y curves for 25 mm diameter pile at depth 75 mm

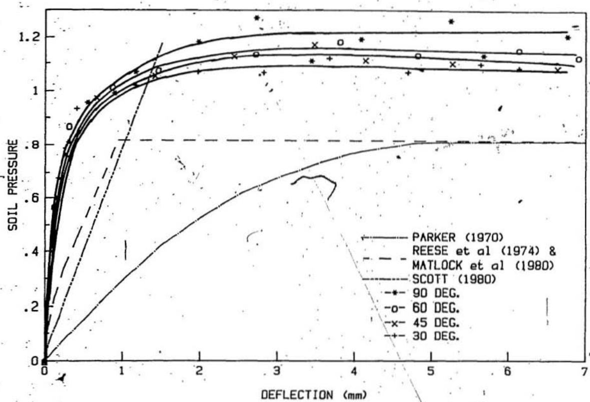

Figure 66: p-y curves for 25 mm diameter pile at depth 100 mm

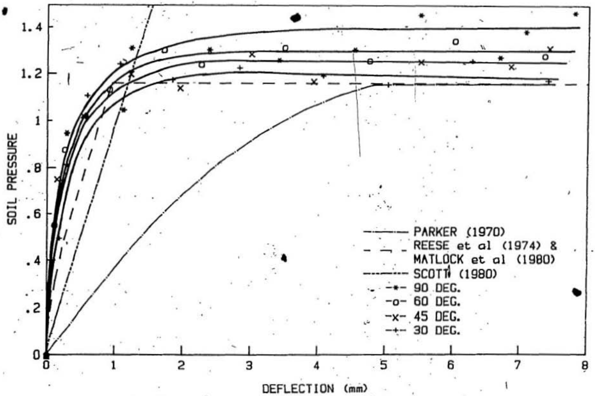

Figure 67: p-y curves for 25 mm diameter pile at depth 125 mm

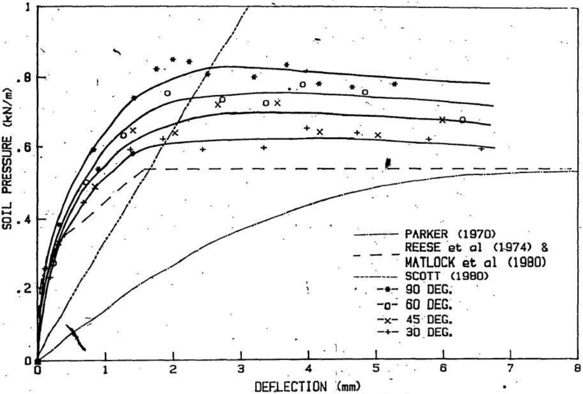

Figure 68: p-y curves for 42 mm diameter pile at depth 42 mm

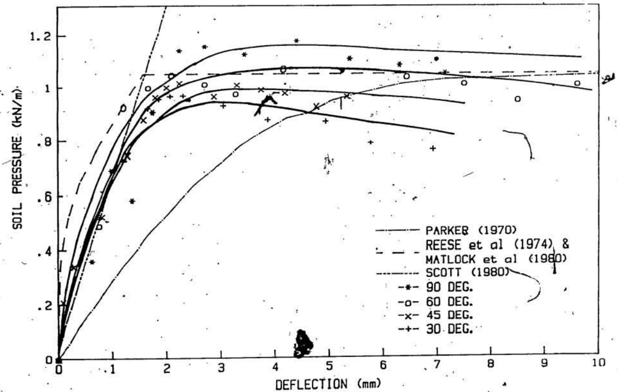

Figure 69: p-y curves for 42 mm diameter pile at depth 84 mm

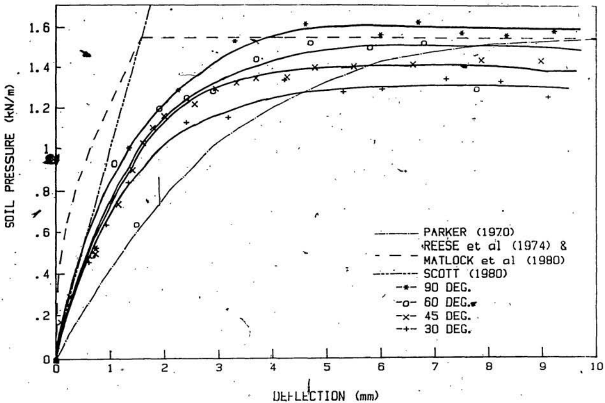

Figure 70: p-y curves for 42 mm diameter pile at depth 126 mm

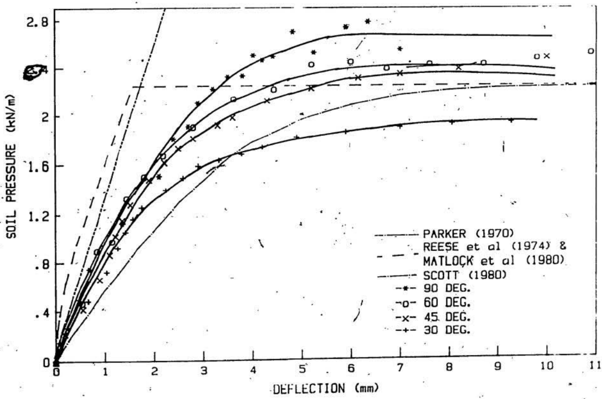

Figure 71: p-y curves for 42 mm diameter pile at depth 168 mm

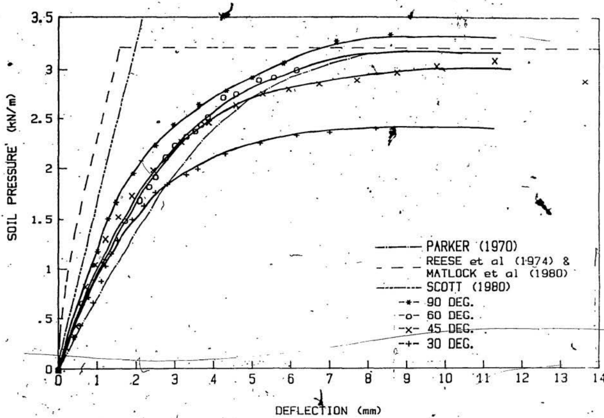

Figure 72: p-y curves for 42 mm diameter pile at depth 210 mm

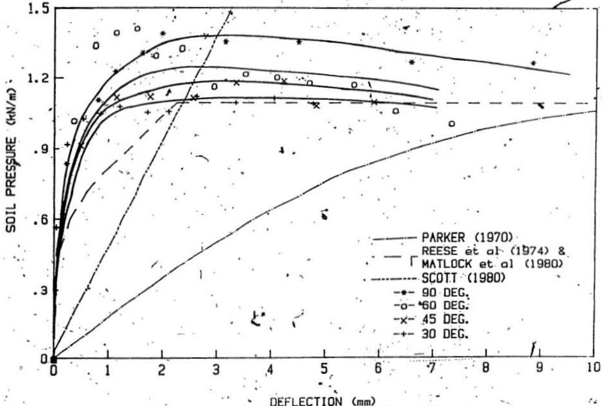

Figure 73: p-y curves for 60 mm diameter pile at depth 60 mm

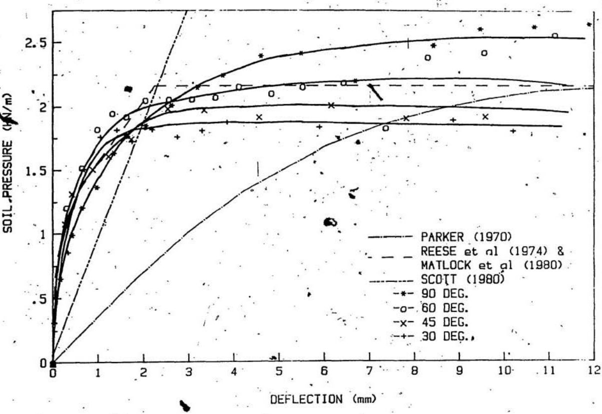

Figure 74: p-y curves for 60 mm diameter pile at depth 120 mm

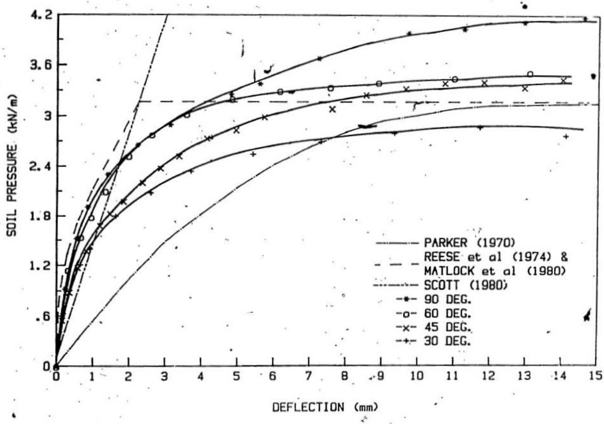

Figure 75: p-y curves for 60 mm diameter pile at depth 180 mm

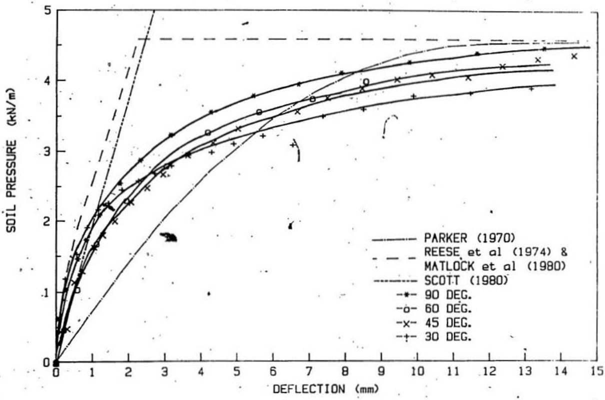

Figure 76: p-y curves for 60 mm diameter pile at depth 240 mm

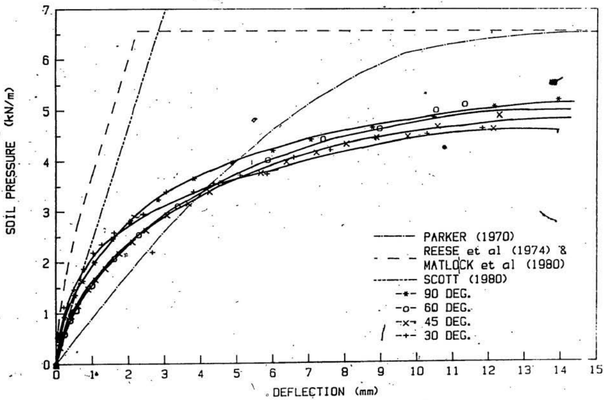

Figure 77: p-y curves for 60 mm diameter pile at depth 300 mm

deflection, whereas in practice, the ultimate resistance is limited by the passive failure of the soil.

It may also be seen that the curves for piles under lateral loading indicated larger soil resistance values than the curves for piles under inclined loading. The values of ultimate soil resistance decreases as load inclination goes from 60 to 30 degrees. These trends are similar to those observed by Parker (1970), where a vertical pile had larger soil resistance values than those of an out-battered pile.

4.5.2 MEASURED AND PREDICTED LATERAL DEFLECTION

During the inclined load tests, the lateral deflection was measured for each load step together with the inclined load. The lateral component of the inclined load was calculated and the corresponding load-deflection curves plotted. The pile behaviour was also computed using the semi-empirical methods of Reese et al (1974), Matlock et al (1980), Scott (1980) and Parker (1970). The pile response was computed as described earlier for the lateral load only.

Comparisons between the measured and predicted load-deformation behaviour of the top of the piles may be made by referring to Figures 78, 79 and 80. It may be noted that for Parker's (1970) method, the predicted deflections are approximately 20 % greater than the measured values for all three piles, especially at lower loads. The method of Reese et al and Matlock et al (1980) agrees fairly well with the measured values underestimating the deflection by about 5%. Scott's (1980) method correctly predicts the deflection values at low loads, but at higher loads underestimates the deflection values by more than a 100 %. It may be concluded that this is because this method does not allow for a limiting value of ultimate soil response to lateral deflection.

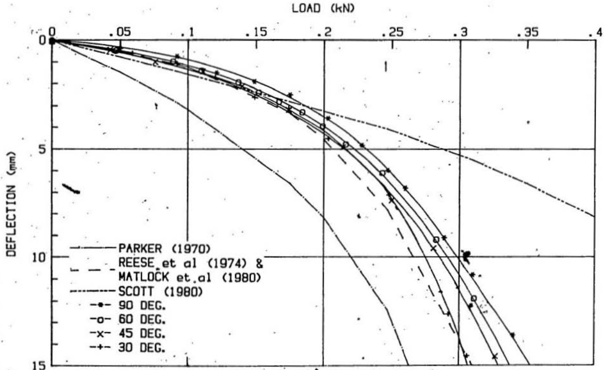

Figure 78: Lateral load-deflection curves for 25 mm diameter pile

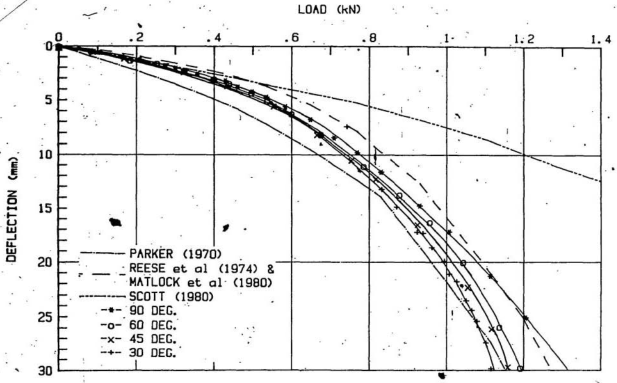

Figure 79: Lateral load-deflection curves for 42 mm diameter pile

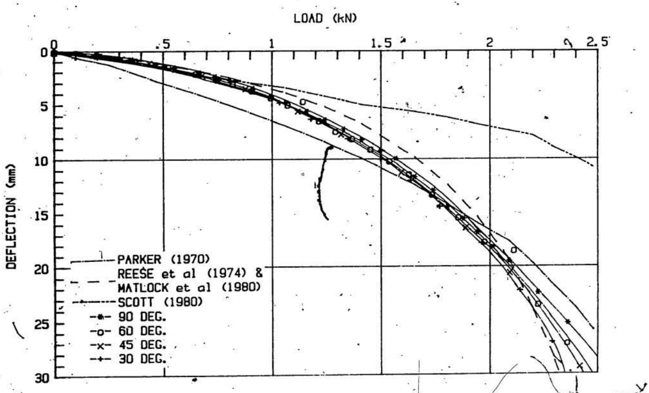

Figure 80: Lateral load-deflection curves for 60 mm diameter pile

It may also be seen that the vertical load on the pile increases the lateral deflection at the pile top. Compared to a pile subjected to the same lateral load only, the vertical load increases the lateral deflections by approximately 4, 9, and 15 % for load inclinations of 60, 45 and 30 degrees respectively at the ultimate lateral load.

4.5.3 MEASURED AND PREDICTED MAXIMUM MOMENT

Comparisons between the measured and predicted lateral load-maximum moment distribution in the pile section, for the piles of diameter 25 mm, 42 mm and 60 mm may be made by referring to Figures 81, 82, and 83. The empirical procedures of Reese et al (1974), Matlock et al (1980), Scott (1980) and Parker (1970) were used to compute the predicted pile response.

It may be seen that at low loads all the methods generally give comparable results and show good agreement with the measured values.

Scott's (1980) method underestimates the maximum moment at higher loads and does not follow the trend exhibited by the measured values. Parker's (1970) method overestimates the moment values but follows the general trend of the measured values. Reese et al (1974) and Matlock et al's (1980) methods show good agreement with the overall trends but underestimate the moment values for the 60 mm pile while overestimating the moment values for the 25 mm and 42 mm diameter piles.

It may also be seen that the addition of a vertical load on the laterally loaded pile increases the maximum moment in the pile section. Compared to a pile subjected to a given lateral load only, the maximum bending moment increases by appoximately 8, 11 and 16% when the pile is subjected to additional vertical loads, with the resultant inclinations of 60, 45, and 30 degrees respec-

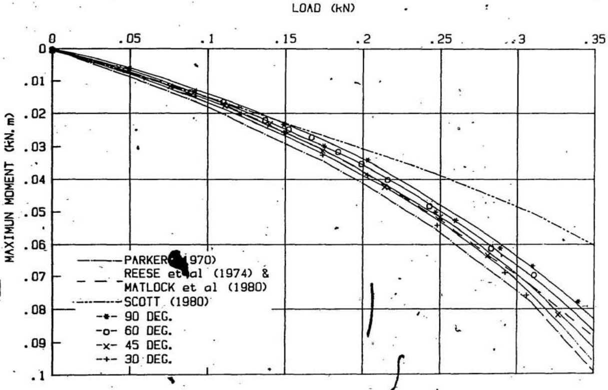

Figure 81: Lateral load-maximum moment curves for 25 mm diameter pile

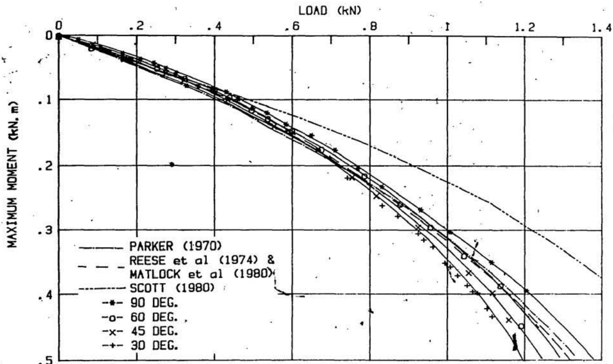

Figure 82: Lateral load-maximum moment curves for 42 mm diameter pile

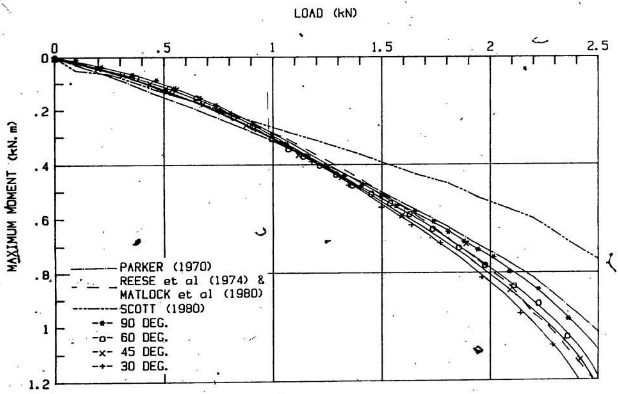

Figure 83: Lateral load-maximum moment curves for 60 mm diameter pile

tively. Hence, the presence of axial load causes additional moment in the pile section which leads to additional lateral deflections as seen in the last section. Similar results have been obtained for long flexible piles by Ramasamy et al (1982), whose analysis shows that the vertical load can increase the lateral deflection by about 7 to 16 % compared to a pile subjected to only lateral load, depending on the degree of fixity of the pile head.

The comparisons between the measured and predicted behaviour of the model piles from the four semi-empirical methods indicate that reasonable results are obtained for sands. It is to be noted that the procedures were originally derived by Parker (1970) and Reese et al (1974) for dense sands. The comparisons here show that the methods are readily applicable to sands with similar properties. It is to be noted that Scott's (1980) criteria of using an unlimited increase in soil response with deflection gives overly conservative results and should be used with caution.

CHAPTER 5

SUMMARY AND CONCLUSIONS

Laboratory experiments were conducted on model vertical flexible piles to better understand the soil-pile interaction under inclined loading in sand. Comparisons were made between experimental and theoretical values. The following conclusions are drawn on the results of this research work.

(1) Cone penetration tests show that fairly uniform conditions are obtained using the raining technique. The critical depth D_c, for the sand was found to be about 17-20 B, consistent with the range of values reported in the literature.

(2) The values of the bearing capacity factor N_q, was constant with depth and consistently smaller than that predicted by various existing theories. The values of N_q compared well with those obtained by Vesic (1977).

(3) Pull out resistance of a vertical smooth pile is estimated as about 75% of the shaft resistance in compression. Theoretical predictions are in significant error when compared with experimental results in predicting the pull out resistance of piles.

(4) Good comparison is obtained between experimental p-y curves and those predicted by Reese et al (1974), Matlock et al (1980), and Parker (1970). Scott's (1980) method differs from the experimental results as his method assumes an unlimited linear increase in soil resistance with increasing deflection. Reese et al (1974), Matlock et al (1980) and Parker (1970) methods are readily applicable to sands with similar properties, where as Scott's (1980) method gives overly conservative results and should be used with caution.

(5) P-y curves for piles under lateral loading indicated larger soil resistance values than curves for piles under inclined loading.

(6) The ultimate load capacity under inclined load decreases with load inclination, with a rapid reduction for load inclinations between 45 and 60 degrees.

(7) The vertical load increases the lateral deflection and maximum moment on the pile under inclined loads. Lateral deflections are increased by about 4-15% and maximum moments by about 8-16% for load inclinations from 30-60 degrees when compared to a pile subjected to the same lateral load only.

REFERENCES

(1) Adams,J.I. and Radhakrishna,H.S.(1973)."The lateral capacity of deep augered footings." 8^{th} Int.Soc.Soil Mech.Vol.3,Moscow,pp1-8.

(2) "API recommended practice for planning, designing and constructing fixed offshore platforms." report RP-2A, American Petroleum Institute, Washinton,D,C.,10^{th} ed.,March 1979.

(3) Awad,A. and Petrasovits,G. (1968). "Considerations on the bearing capacity of vertical and batter piles subjected to forces acting in different directions." Proc. 3^{rd} Conf.S.M. & F.E.,Budapest, pp.484-497.

(4) Banerjee,P.K. and Davies,T.G. (1978). "The behaviour of axially and laterally loaded single piles embedded in nonhomogeneous soils." Geotechnique, Vol. 28, No. 3, pp.309-326.

(5) Barton,Y.O.,Finn,W.D.L.,Parry,R.H.S. and Towhata,I.(1983). "Lateral pile response and p-y curves from centrifuge tests." 15^{th} Off. Tech. Conf., Houston,Texas, Paper # 4502.

(6) BCP Committee (1971). "Field tests on piles in sand." Soils and Foundations, Vol. 11, No. 2, pp.29-41.

(7) Berezantzev,V,G.,Khristoforov,V.S. and Golubkov,V,N.(1961)."Load bearingcapacity and deformation of piled foundations." Proc. 5^{th} Int.conf.S.M. & F.E.,Vol.2,pp.11-15.

(8) Bieganousky,W.A. and Marcuson,W.F.(1976). "Uniform placement of sand." ASCE,Vol.102,No.GT3,pp.229-233.

(9) Bolton,M.D. (1984). "The strength and dilatancy of sands." Cambridge Univ. Eng. Dept. Res. Report, CUED/D-Soils TR 152.

(10) Brinch Hansen,J.(1951)."Simple statical computation of permissible pile loads." Christiani and Nielsen Post,pp.14-17.

(11) Brinch Hansen,J.(1961). "The ultimate resistance of rigid piles against transversal forces." Danish Geotechnical Institute,Bul.No. 12,Copenhagen,pp.5-9.

(12) Broms,Bengt B. and Silgerman,orge O.(1964). "Skin friction resistance for piles in cohesionless soils." Sols Soils,Vol.3,No.10,pp.33-43.

(13) Broms,Bengt B.(1964). "Lateral resistance of piles in cohesionless soils." ASCE Vol.90,No.SM3,pp.123-156.

(14) Broms Bengt B.(1965). "Piles in cohesionless soils subjected to oblique pull." ASCE Vol.91,No.SM4,pp.199-205.

(15) Broms Bengt B.(1966). "Methods of calculating the ultimate bearing capacity of piles, a summary." Sols Soils,No.18-19,pp.21-31.

(16) Broms,Bengt B. (1972). "Stability of flexible structures (Piles and pile groups)." Proc. 5^{th} Eur. Conf. Soil Mech. Fndn. Eng., Madrid, Vol. 2, pp. 239-269.

(17) Chari,T.R. and Meyerhof,G.G.(1983). "Ultimate capacity of rigid single pile under inclined loads in sand." Can. Geotech. J.,Vol.20, pp.849-854.

(18) Chaudhuri,K.P.R. and Symons,M.V. (1983). "Uplift resistance of model single piles." Proc. of the Conf. on Geotech. practice in Off. Eng., ASCE, Austin, Texas, pp. 335-355.

(19) Cox,W.R.,Reese,L.C. and Grubbs,B.R. (1974) "Field testing of laterally loaded piles in sand." 6th Off. Tech. Conf., Houston, Texas, Paper # 2079.

(20) Coyle,H.M. and Castello,R.R.(1979). "A new look at bearing capacity factors for piles." 11th Offshore Tech. Con.,Houston' pp.427-435.

(21) Davisson,M.T. and Prakash,S. (1963) "A review of soil pile behaviour." High. Res. Rec., No. 39, pp. 25-48.

(22) Davisson,M.T. and Mitchell,J.K.(1973). "Static penetration resistance of soil." Space Sciences Laboratory Series 14,Issue 24, Univ. of Cal.

(23) Douglas,D.J. and Davis,E.H. (1964). "The movement of buried footings due to moment and horizontal load and the movement of anchor plates." Geotechnique, Vol. 14, No. 2, PP.115-132.

(24) Evans,L.T.(1953). "Bearing piles subjected to horizontal loads." ASTM STP 154,pp.30-37.

(25) Fleming,W.G.K. and Thorburn,S. (1983). "Recent piling advances, State of the art report." in Proc. Conf. on Advances in Piling and Ground Treatement for Foundations, ICE, London.

(26) Fleming,W.G.K., Weltman,A.J., Randolph,M.F. and Elson,W.K. (1985). "Piling Engineering." John Wiley & Sons, Inc., New York.

(27) Focht,J.A., and McClelland, B. (1955). "Analysis of laterally loaded piles by difference equation solution." The Texas Engineer, Texas Section, ASCE.

(28) Gleser,S.M. (1954). "Lateral load tests on vertical fixed head and free head piles." , ASTM STP 154, pp.75-93.

(29) Hanna,T.H. and Tan,R.H.S. (1973). "The behaviour of long piles under compressive loads in sand." Can. Geotech. J.,Vol. 10, No. 3, pp. 311-340.

(30) Hetenyi,M. (1946). "Beams on elastic foundation." University of Michigan Press, Ann Arbor, Michigan.

(31) Horvath,J.S. (1984). "Simplified Elastic continuum applied to the laterally loaded pile problem-Part 1:Theory." Laterally loaded deep foundations: Analysis and performance, ASTM STP 835,pp.112-121.

(32) Howe,R.J. (1955). "A numerical method for predicting the behaviour of laterally loaded piling." EPR Publication 412, Shell Development Co., Houston, Texas.

(33) Hunter,A.H. and Davisson, M.T. (1969). "Measurement of pile load transfer." Performance of deep foundations, ASTM STP 444, pp. 106-117.

(34) Ireland,H.O. (1957). "Pulling tests on piles in sand." Proc. 4th Int. Conf. Soil Mech., London, England, pp. 43-45.

(35) Ismael,N.F. and Klym,T.W. (1978). "Behaviour of rigid piers in layered cohesive soils." ASCE Vol.104,GT8,pp.1061-1074.

(36) Ismael,N.F. and Klym,T.W. (1979). "Uplift and bearing capacity of short piers in sand." J. of Geotech. Eng., ASCE, Vol. 105, No. GT5, pp. 579-593.

(37) Joo,J. (1985) "Behaviour of large scale rigid model piles under inclined loads in sand." MEng. Thesis, Memorial Univ. of Nfld. St. John's, Nfld, 135pp.

(38) Kerisel,J.(1964). "Deep foundations basic experimental facts." Proc. of the North American

Conf. on Deep Foundations, Mexico, Vol. 1, pp.5-44.

(39) Kishida,H. (1963). "Stress distribution by model piles in sand." Soils and Foundations, Vol. 4, No. 1, pp.1-23.

(40) Kishida,H. and Meyerhof,G.G. (1965). "Bearing capacity of pile groups under eccentric loads in sand." Proc. 5^{th} Int. Conf. Soil Mech., Vol. 2, pp.270-274.

(41) Levacher,D.R., and Sieffert, J.G. (1984). "Tests on model tension piles." J. of Geotech. Eng.,ASCE, Vol. 110, No. 12, pp. 1735-1748.

(42) Madhav,M.R., Kameswara Rao, N.S. and Madhavan,K. (1971). "Laterally loaded piles in elastoplastic soil." Soils and Foundation, Vol. 11, No. 2, Tokyo.

(43) Madhav,M.R. and Sarma,C.R.K. "Analysis of axially and laterally loaded long pile." Proc. 2^{nd} Int. Conf. on Num. Meth. in Off. Piling." April 1982, pp.577-596.

(44) Matlock,H. and Ripperger,E.A. (1956). "Procedures and Instrumentation for tests on a laterally loaded pile." Proc. 8^{th} Texas Conf. on S.M. and F.E.,Austin, Texas, 1956.

(45) Matlock,H. and Reese,L.C. (1962). "Generalized solutions for laterally loaded piles." ASCE, Transactions, Vol. 127, Part 1, pp.1220-1251.

(46) Matlock,H. (1970). "Correlations for design of laterally loaded piles in soft clay." Paper # Otc 1204, Proc. 2^{nd} Off. Tech. Conf., Houston, Texas.

(47) Matlock,H. and Lam,I. (1980). "Design of pile foundations." Int. Symp. on Marine Soil Mech., Mexico City, pp.55-69.

(48) McClelland,B. and Focht,J.A. (1958). "Soil modulus for laterally loaded piles." Trans. ASCE, Vol. 123, paper No. 2954, pp.1049-1086.

(49) McClelland,B. and Focht,J.A. (1967). "Problems in design and installation of heavily loaded pipe piles." ASCE Proc. of Conf. on Civil Eng. in the Oceans, pp.601-634.

(50) Meyerhof,G.G. (1951). "The ultimate bearing capacity of foundations." Geotechnique, Vol. 2, pp.301-332.

(51) Meyerhof,G.G. (1953). "The bearing capacity of foundations under eccentric and inclined loads." Proc. 3^{rd} Int. Conf. on S. M. and F. E., Vol. 1, session 4/24, Switzerland, pp.440-445.

(52) Meyerhof,G.G. (1956). "Penetration tests and bearing capacity of piles." ASCE, Vol. 82, No. SM1, pp.1-19.

(53) Meyerhof,G.G. and Ranjan,G. (1972). "The bearing capacity of rigid piles under inclined loads in sand. 1: vertical piles." Can. Geotech. J. Vol. 9, pp.430-446.

(54) Meyerhof,G.G. (1973). "The uplift capacity of foundations under oblique loads." Can. Geotech. J. Vol. 10, pp. 64-70.

(55) Meyerhof,G.G. (1976). "Bearing capacity and settlement of pile foundations." ASCE, Vol. 102, No. GT3, pp.197-228.

(56) Meyerhof,G.G., Mathur, S.K., and Valsangkar,A.J. (1981). "The bearing capacity of rigid piles and pile groups under inclined loads in layered sand." Can. Geotech. J., Vol. 18, pp. 514-519.

(57) Meyerhof,G.G., Yalcin,A.S. and Mathur,S.K. (1983). "Ultimate pile capacity for eccentric in-

clined load." J. of Geotech. Eng., Vol. 109, No. 3, pp. 408-423.

(58) Mindlin,R.D. (1936). "Force at the point in the interior at a semi-infinite solid." Physics No. 5, pp 195-202.

(59) Mohan,D., Jain,G.S. and Kumar,U. (1963). "Load bearing capacity of piles." Geotechnique, Vol. 13, No. 1, pp. 76-86.

(60) Mori,H. (1964). "The behaviour of pipe piles under vertical and horizontal load." Proc. Symp. on Bearing Capacity of Piles, New Delhi.

(61) Morgan,J.R. and Poulos,H.G. (1968). "Settlement and stability of deep foundations." in Soil Mechanics-Selected Topics, ed. I.K. Lee. Sydney, Aust.: Butterworths: pp.528-609.

(62) Mustafayev,A.A., Mamedov,K.M. and Ismailov,B.G. (1972). "Pipe filling piles of sea oilfield structures and methods of calculation of lateral forces." Proc. 5th European Conf. on S.M. and F.E., Madrid, pp.381-386.

(63) Muzas,F. (1972). "Contribution to the study of laterally loaded piles." Proc. 5th European Conf. on S.M. and F.E., Madrid, pp.387-396.

(64) Nordlund,R.L. (1963). "Bearing capacity of piles in cohesionless soils." ASCE, Vol. 89, No. SM3, PP.1-35.

(65) Palmer,L.A. and Thompson,J.B. (1948). "The earth pressures and deflections along the embedded lengths of piles subjected to lateral thrust." Proc. 2rd Int. Conf. on S.M. and F.E., Vol. V, pp.156-161.

(66) Parker,F.Jr. and Reese,L.C. (1970). "Experimental and Analytical studies of behaviour of single piles in sand under lateral and axial loading." Res. Report No. 117-2, The Texas Highway Dept. 250 pp.

(67) Petrasovits, G. and Awad, A. (1972). "Ultimate lateral resistance of a rigid pile in cohesionless soil." 5th Eur. Conf. on S. M. & F. E., Vol. 1, pp. 407-412.

(68) Pise,P.J. (1977). "Experimental coefficients for laterally loaded piles." Int. Symp. on Soil Structure Interaction, U. of Roorkee, Rorokee, India, pp.145-150.

(69) Pontyondy,J.G. (1961). "Skin friction between various soils and construction materials." Geotechnique, Vol. 11, No. 4, pp.339-353.

(70) Poulos,H.G. (1971). "Behaviour of laterally loaded piles: 1- single piles." ASCE, Vol. 97, No. SM5, pp.711-731.

(71) Poulos,H.G. and Davis,E.H. (1980). "Pile foundation analysis and design"." John Wiley & Sons.

(72) Prandtle,L. (1920). "On the hardness of plastic bodies." Nachr. Kgl. Ges. Wiss Gottingen, Math-Phys. Kl.

(73) Randolph,M.F. (1981). "The response of flexible piles to lateral loading." Geotechnique, Vol. 31, No. 2, pp. 247-259.

(74) Reddy,A.S. and Ramasamy,G. (1973). "Analysis of an axially and laterally loaded tapered pile in sand." Soils and Foundations, Vol. 13, No. 4 pp.15-27.

(75) Reddy,A.S. and Valsangkar,A.J. (1968). "An analytical solution for laterally loaded piles in layered soils." Sols Soils, No. 21, pp. 23-28.

(76) Reddy,A.S. and Valsangkar,A.J. (1970). "Generalized solutions for laterally loaded piles on elasto-plastic ground." Soils and foundation, Vol. 10, No. 3, Tokyo, pp.66-80.

(77) Reese,L.C. (1975a). "Laterally loaded piles." GESA Report No. D-75-14, UCC Report No. 75-14, Geotechnical Engineering Software Activity, Univ. of Colorado Computing Cen., Boulder, Colorado.

(78) Reese,L.C. (1975b). "Analysis of laterally loaded piles-Software documentation." GESA Report No. D-75-7, UCCC Report No. 75-10, Dep. of Civil Eng., Univ. of Texas at Austin, Texas.

(79) Reese,L.C. (1977). "Laterally loaded piles : Program documentation." ASCE, Vol. 103, GT4, pp.287-305.

(80) Reese,L.C. Cox,W.R. and Koop,F.D. (1974). "Analysis of laterally loaded piles in sand." 6th Off. Tech. Conf., Houston, Texas, Paper No. 2080.

(81) Reese,L.C. and Ginzbarg,A.S. (1958). "Difference equation method for laterally loaded piles with abrupt changes in flexural rigidity." EPR Memo. Report 39, Shell Development Company, Houston, Texas.

(82) Reese,L.C. and Manoliu,H. (1973). "Analysis of laterally loaded piles by computer." Buletinul Stiintific, Al Institutului de Constructii Bucuresti, Anul XVI, NR. 1, pp.35-70.

(83) Reese,L.C. and Matlock,H. (1956). "Non-dimensional solutions for laterally loaded piles with soil modulus assumed proportional to depth." Proc. 8th Texas Conf. on S.M. and F.E., Austin, Texas.

(84) Reissener,H. (1924). "The earth pressure problem." Proc. 1st Int. Conf. Appl. Mech.

(85) Sanglerat,G. (1972). "The Penetrometer and soil exploration." Elsevier, Amsterdam, 464 pp.

(86) Sogge,R.L. (1981) "Laterally loaded pile design." J. of Geotech. Eng., ASCE, Vol. 107, No. GT9, pp.1179-1193.

(87) Sowa,V.A. (1970). "Pulling capacity of concrete cast in-situ bored piles." Can. Geotech. J., Vol. 7, pp. 482-493.

(88) Spillers,W.R., and Stoll,R.D., (1964). "Lateral response of piles." ASCE Vol. 90, SM6, pp.1-9.

(89) Sullivan,W.R., Reese,L.c. and Fenske,C.W. (1979). "Unified method for analysis of laterally loaded piles in clay." Conf. on Num. methods in Offshore Piling." Inst. of Civil Engs., London, pp. 135-146.

(90) Tavenas,F.A. (1970). "Load test results on friction piles in sand." Can. Geotech. J., Vol. 8, pp. 7-22.

(91) Terzaghi,K. (1943). "Theoretical soil mechanics." John Wiley and sons, New York.

(92) Terzaghi,K. (1955). "Evaluation of coefficient of subgrade reaction." Geotechnique, Vol. 5, No. 4, pp.297-326.

(93) Tomlinson,M.J. (1977). "Pile design and construction practice." A Viewpoint Publication.

(94) Toolan,F.E. and Horsnell,M.R. (1979). "Analysis of the load-deflexion behaviour of offshore piles and pile groups." Num. Meth. in Off. Piling, Ins. of Civil Eng., London, pp. 147-155.

(95) Valsangkar,A.J.,Kameswara Rao,N.S.V. and Basudhar,P.K. (1973). "Generalized solutions of axially and laterally loaded piles in elasto-plastic soil." Soils and Foundations, Vol. 13, No. 4, pp.

1-14.

(96) Vesic, A.S. (1963). "Bearing capacity of deep foundations in sand." Highway Res. Rec. No. 39, pp.112-153.

(97) Vesic, A.S. (1967). "Ultimate loads and settlements of deep foundations in sand." Proc. of Symposium on bearing capacity and settlement of foundations. Duke University, pp.53-68.

(98) Vesic, A.S. (1970). "Tests on instrumented piles, Ogeechee River Site." J. of S. Mech. Found. Eng., ASCE, Vol. 96, No. 2, pp. 561-584.

(99) Vesic, A.S. (1972). "Expansion of cavities in infinite soil mass." ASCE, Vol. 98, No. SM3, pp.265-290.

(100) Yakoyama (1985). "A non-linear analysis of pile structures." Soils and foundations, Vol. 25, No. 4, pp.92-102.

(101) Yoshimi, Y. (1964). "Piles in cohesionless soil subject to oblique pull." ASCE, Vol. 90, No. SM6, pp.11-24.

APPENDIX A

COMPUTER PROGRAMS

```
10    REM*********************CPTEST PROGRAM***********************
20    ! PROGRAM TO CONDUCT CONE PENETRATION TESTS
30    OPTION BASE 1
40    DIM BDATA$[156],A$[99],PENT(10),MULTPLX(90),PENTAVG(25),D(25),
.     LOADS(25),LOADAVG(25),CONAVG(25),SLVAVG(25),VINAVG(25)
50    PRINTER IS 1
60    CREATE "CPTD17",5,256
70    ! SLEEVE IS CONNECTED TO CHANNEL 67
80    ! CONE IS CONNECTED TO CHANNEL 68
90    ! LOAD CELL IS CONNECTED TO CHANNEL 69
100   ! INPUT VOLTAGE IS READ ON CHANNEL 70
110   ! START TEST TAKING 10 READINGS PER CHANNEL
120   DISP "INPUT NUMBER OF READINGS TO BE TAKEN"
130   INPUT NUMLR
140   FOR J=1 TO NUMLR
150   DISP "INPUT DEPTH D"
160   INPUT D(J)
170   DISP "PRESS [CONT] TO TAKE READINGS FOR NEW DEPTH"
180   PAUSE
190   ! READ DATA
200   DISP "******READING DATA FROM 3497A******"
210   IOBUFFER BDATA$
220   CLEAR 509
220   OUTPUT 509 ;"VF2VA0VR5VT2SD1"
230   OUTPUT 509 ;"SO1VN1AF67AL70AE1AC67"
240   DISP "DATA GOING IN, HANG ON !"
250   ! NOW TRANSFER DATA TO FILE USING FHS
260   TRANSFER 509 TO BDATA$ FHS
270   LOCAL 509 @ CLEAR 509 @ BEEP 10,100
280   DISP "DATA TRANSFER COMPLETE"
290   NDP=10
300   ! DO NOT STORE DATA BEFORE UNPACKING"
310   !********UNPACKING DATA********
320   DISP "UNPACKING DATA , PLEASE WAIT"
330   FOR I=3 TO 12*NDP STEP 3
340   A$=DTB$ (NUM (BDATA$[I-2,I-2]))
350   D$=A$
360   A2=BINAND (BTD (A$[9,10]),3)
370   M=10^(-6+A2)  ! RANGE MULTIPLIER
380   IF BINAND (BTD (A$[11,11]),1)=1 THEN SIGN=-1 ELSE SIGN=1
390   ORNG=BINAND (BTD (A$[12,12]),1)
400   MSD=BINAND (BTD (A$[13,16]),15)
410   A$=DTB$ (NUM (BDATA$[I-1,I-1]))
420   B$=A$
```

```
430   SSD=BINAND (BTD (A$[9,12]),15)
440   TSD=BINAND (BTD (A$[13,16]),15)
450   A$=DTB$ (NUM (BDATA$[1,1]))
460   C$=DTB$ (NUM (BDATA$[I,I]))
470   FSD=BINAND (BTD (A$[9,12]),15)
480   LSD=BINAND (BTD (A$[13,16]),15)
490   IF I=9 THEN DISP D$,B$,C$
500   MULTPLX(I/3)=(ORNG*10^5+MSD*10^4+SSD*10^3+TSD*10^2+
      FSD*10+LSD)*M*SIGN
510   NEXT I
520   !********DEMULTPLEX********
530   C1=1 @ N=NDP
540   FOR I=1 TO NDP
550   LOADS(I)=MULTPLX(C1)   @ C1=C1+1
560   LOADCON(I)=MULTPLX(C1) @ C1=C1+1
570   LOADSLV(I)=MULTPLX(C1) @ C1=C1+1
580   VIN(I)=MULTPLX(C1)     @ C1=C1+1
590   NEXT I
600   ! DISP THE DATA FOR CHECKING PURPOSES
610   DISP "STATIC CONE PENETROMETER"
620   FOR I=1 TO NDP
630   PRINT USING 640 ; LOADSLV(I),LOADCON(I),LOADS(I),VIN(I)
640   IMAGE 10X,3D.6DD,3X,3D.6DD,3X,3D.6DD,3X,3D.6DD
650   NEXT I
660   ! FIND THE AVERAGE VALUE FOR STORAGE
670   LOADSLV(0)=0 @ LOADCON(0)=0 @ LOADS(0)=0 @ VIN(0)=0
680   FOR I=1 TO NDP
690   LOADSLV(I)=LOADSLV(I-1)+LOADSLV(I)
700   LOADCON(I)=LOADCON(I-1)+LOADCON(I)
710   LOADS(I)=LOADS(I-1)+LOADS(I)
720   VIN(I)=VIN(I-1)+VIN(I)
730   NEXT I
740   SLVAVG(J)=LOADSLV(NDP)/NDP
750   CONAVG(J)=LOADCON(NDP)/NDP
760   LOADAVG(J)=LOADS(NDP)/NDP
770   VINAVG(J)=VIN(NDP)/NDP
780   NEXT J
790   ! STORE DATA IN DATA FILE
800   ASSIGN# 1 TO "CPTD17"
810   PRINT# 1 ; D(),SLVAVG(),CONAVG(),LOADAVG(),VINAVG()
820   ASSIGN# 1 TO *
830   DISP "PROGRAM RUN FINISHED"
840   END
```

```
10   REM PYCURVES PLOTTING SUBROUTINE
20   DISP "ENTER PLOTTER ADDRESS 1,505"
30   INPUT PL
40   PLOTTER IS PL
50   OPTION BASE 1
60   DIM X(30),Y(30)
70   GCLEAR
80   LOCATE 20,120,22.5,87.5
90   CLEAR
100  FXD 2,0
110  CSIZE 3
120  DISP "ENTER SCALE IN FORM   XMIN,XMAX,YMIN,YMAX"
130  INPUT XMIN,XMAX,YMIN,YMAX
140  SCALE XMIN,XMAX,YMIN,YMAX
150  AXES 1,.2,0,0,1,2,3
160  FOR Y=0 TO YMAX 1 STEP .2
170  LDIR 0 @ LORG 8
180  MOVE 0,Y
190  LABEL Y
200  NEXT Y
210  FOR X=0 TO XMAX
220  LDIR 0 @ LORG 4
230  MOVE X,-(.04*YMAX)
240  LABEL X
250  NEXT X
260  X1=XMAX/8
270  X2=YMAX/1
280  MOVE 6.5*X1,.34*X2
290  LABEL "PARKER (1970)        "
300  MOVE 6.5*X1,.3*X2
310  LABEL "REESE et al (1974) &"
320  MOVE 6.5*X1,.26*X2
330  LABEL "MATLOCK et al (1980)"
340  MOVE 6.5*X1,.22*X2
350  LABEL "SCOTT (1980)         "
360  MOVE 5.6*X1,.18*X2
370  LABEL "-*- 90 DEG."
380  MOVE 5.6*X1,.14*X2
390  LABEL "-o- 60 DEG."
400  MOVE 5.6*X1,.1*X2
410  LABEL "-x- 45 DEG."
420  MOVE 5.6*X1,.06*X2
430  LABEL "-+- 30 DEG."
440  FRAME
```

```
450   CLEAR
460   REM ***READ DATA FROM DISC***
470   DISP "INPUT FILE NAME OF POINTS TO BE PLOTTED"
480   INPUT FIL$
490   ASSIGN# 1 TO FIL$
500   READ# 1 ; X(),Y()
510   ASSIGN# 1 TO *
520   DISP "HOW MANY POINTS TO BE PLOTTED"
530   INPUT POINT
540   DISP POINT,"POINTS ENTERED"
550   BEEP 50,300
560   MOVE X(1),Y(1)
570   LORG 5
580   DISP "INPUT TYPE OF PLOT TO BE PLOTTED, LINR OR OTHERWISE,
      LINE/1,OTHER/2"
590   INPUT ANS
600   IF ANS=1 THEN GOTO 680
610   DISP "INPUT TYPE OF PLOT *,o,+, etc "
620   INPUT CAR$
630   FOR I=1 TO POINT
640   MOVE X(I),Y(I)
650   LABEL CAR$
660   NEXT I
670   GOTO 770
680   DISP "ENTER LINE TYPE 1 TO 8"
690   INPUT LIN
700   FOR I=1 TO POINT
710   LINE TYPE LIN
720   DRAW X(I),Y(I)
730   NEXT I
740   DISP "REPLOT SAME NUMBERS WITH DIFFERENT PLOT Y/N"
750   INPUT AN$
760   IF AN$="Y" THEN GOTO 610
770   DISP "DO YOU WANT TO PLOT ANOTHER CURVE ON THIS GRAPH Y/N"
780   INPUT ANS$
790   IF ANS$="Y" THEN GOTO 470
800   DEG
810   DISP "DO YOU WANT TO LABEL GRAPH, INPUT Y/N"
820   INPUT ANS$
830   IF ANS$="N" THEN GOTO 1030
840   DISP "HORIZONTAL OR VERTICAL LABELS H/V"
850   INPUT LAB$
860   IF LAB$="H" THEN GOTO 890
870   LDIR 90
```

```
880    GOTO 900
890    LDIR 0
900    DISP "ENTER SIZE OF LETTERING, 1 SMALL, 10 LARGE"
910    INPUT SI
920    CSIZE SI
930    DISP "ENTER LORG VALUE, 1-9, 1-3 RIGHT JUSTIFIED,
       4-6 CENTERED, 7-9 LEFT JUSTIFIED"
940    INPUT LOR
950    LORG LOR
960    DISP "ENTER COORDINATES FOR LABEL TO BE CENTERED ON"
970    INPUT X,Y
980    MOVE X,Y
990    DISP "ENTER LABEL"
1000   INPUT LAB$
1010   LABEL LAB$
1020   GOTO 810
1030   BEEP
1040   DISP "IF YOU WANT TO RUN PROGRAM AGAIN TYPE Y"
1050   INPUT RUN$
1060   IF RUN$="Y" THEN GOTO 10
1070   DISP "PROGRAM FINISHED"
1080   BEEP 50,300 @ BEEP 25,300
1090   END
```

```
C     ****************************************************************
C     PROGRAM TO CALCULATE PILE DEFLECTION, SHEAR, SLOPE AND SOIL
C     PRESSURE FROM GIVEN MOMENT DIAGRAM USING SIMPSON'S RULE
C     X - GAUGE LOCATION
C     Y - BENDING MOMENT
C     ****************************************************************
      DIMENSION X(25),Y(25),F(25,15),FT(15,25),A(15,16),B(15),C(15)
      DIMENSION XLC(201),YLC(201),XINT(201),YINT(201),AREA(201)
      DIMENSION P(201),SPRE(201),SHEAR(201),PRE(201)
C
C     DEFINE THE FUNCTIONS
      F1(X)=1.0
      F2(X)=X
      F3(X)=X*X
      F4(X)=X**3
      F5(X)=X**4
      F6(X)=X**5
      F7(X)=X**6
      F8(X)=X**7
      DUMMYF(X)=C(1)+C(2)*X+C(3)*X*X+C(4)*X**3+C(5)*X**4+C(6)*X**5+C(7)*
     &X**6
      DUMMYP(X)=(C(2)+2*C(3)*X+3*C(4)*X*X+4*C(5)*X**3+5*C(6)*X**4+6*C(7)
     &*X**5)
      DUMMYL(X)=(2*C(3)+6*C(4)*X+12*C(5)*X*X+20*C(6)*X**3+30*C(7)*X**4)
C
C     READ IN THE NUMBER OF C'S AND NUMBER OF DATA POINTS
      READ(3,*)M,N
      NUM=100
C
C     READ X-Y VALUES OF DATA POINTS
      READ (3,*) (X(I),Y(I),I=1,N)
      READ (3,*) EI
C
      WRITE(2,600)
      XI=X(1)
      XL=X(N)
      WRITE(2,500) (X(I),Y(I),I=1,N)
  600 FORMAT (/15X,' INPUT DATA ',//15X, 'X',7X,'Y')
  500 FORMAT (10X,F8.3,5X,F8.3)
C     GENERATE THE F MATRIX
      DO 4 I=1,N
      F(I,1)=F1(X(I))
      F(I,2)=F2(X(I))
      F(I,3)=F3(X(I))
```

```
      F(I,4)=F4(X(I))
      F(I,5)=F5(X(I))
      F(I,6)=F6(X(I))
    4 F(I,7)=F7(X(I))
C
C     GENERATE THE TRANSPOSE OF THE F MATRIX
      DO 5 I=1,N
      DO 5 J=1,M
    5 FT(J,I)=F(I,J)
C
C     DETERMINE COEFFICIENT MATRIX A OF SIMULTANOUS EQUATION SYSTEM
      CALL MATMPY(FT,F,A,M,N,M)
C
C     DETERMINE THE COLUMN OF CONSTANTS FOR SIMULTANEOUS
C     EQUATION SYSTEM
      CALL MATMPY(FT,Y,B,M,N,1)
      DO 6 I=1,M
    6 A(I,M+1)=B(I)
C     DETERMINE C VALUES BY SOLVING SIMULTANEOUS EQUATIONS
C     USING CHOLESKY METHOD
      MP1=M+1
      CALL CHLSKY(A,M,MP1,C)
C
C     WRITE OUT THE C VALUES
      WRITE(2,7)
    7 FORMAT('1',4X,'C(1) THROUGH C(M)'/)
      WRITE(2,8) (I,C(I),I=1,M)
    8 FORMAT(' ',3X,'C(',I1,')=',E14.7)
C     CALCULATION OF THE CURVE ORDINATES
      XINC=(XL-XI)/NUM
      JL=NUM+1
      DO 700 K=1,JL
      XLC(K)=XI+(K-1)*XINC
      YLC(K)=DUMMYF(XLC(K))
  700 CONTINUE
      WRITE(2,800)
  800 FORMAT(/5X,'TABULATED VALUES OF THE FITTED CURVE',/15X,
     *'POINT #',5X,'X VARIABLE',3X,'Y VARIABLE'/)
      DO 1000 K=1,JL
      WRITE(2,900) K,XLC(K),YLC(K)
  900 FORMAT(15X,I3,2X,F10.3,2X,F10.3)
 1000 CONTINUE
C*********INTEGRATE MOMENT CURVE TO OBTAIN SLOPE*************
      M=50
```

```
      N=M-1
      K=1
      XMAX=XL
      DH=XMAX/201.0
      XMIN=XMAX-DH
      DO 85 J=1,201
      H=(XMAX-XMIN)/N
      SUM=0.0
      XN=XMIN+H
      DO 14 I=2,N
      IF (MOD(I,2)) 12,12,13
   12 SUM=SUM+4.*DUMMYF(XN)
      GO TO 14
   13 SUM=SUM+2.*DUMMYF(XN)
   14 XN=XN+H
      AREA(K)=H/3.*(DUMMYF(XMIN)+SUM+DUMMYF(XMAX))
C     WRITE(1,*) XMIN,AREA(K)
      XMIN=XMIN-DH
      K=K+1
   85 CONTINUE
C*****INTEGRATE FUNCTION AGAIN TO OBTAIN DEFLECTION***********
      XDUM=0.0
      N=201
      DO 95 J=1,67
      M=N-1
      K=M-1
      H=DH
      SUMEV=0.0
      SUMOD=0.0
      DO 15 I=2,M,2
   15 SUMEV=SUMEV+AREA(I)
      DO 16 I=3,K,2
   16 SUMOD=SUMOD+AREA(I)
      YINT(J)=1000.0*((H/3.)*(AREA(1)+4.*SUMEV+2.*SUMOD+AREA(N)))/EI
C     WRITE(1,*) XDUM,YINT(J)
      XDUM=XDUM+(3.*DH)
      N=N-3
   95 CONTINUE
      XINC=(XL/201.)*3.
      WRITE(1,430)
  430 FORMAT ('*******PILE TWO ALPHA=90 DEGREES DEG OF POLY=7 ***')
      WRITE(1,440)
  440 FORMAT('      DEP          DEF          SHEAR          SPR          SLOPE
     &   SHEAR          SPR')
```

```
      DO 760 K=1,68
      XLC(K)=XI+(K-1)*XINC
      YLC(K)=DUMMYF(XLC(K))
  760 CONTINUE
      P(1)=((4.*YLC(2)-YLC(3)-3.*YLC(1))/(2.*XINC))
      P(2)=((4.*YLC(3)-YLC(4)-3.*YLC(2))/(2.*XINC))
      PRE(1)=((4.*YLC(3)-YLC(4)-5.*YLC(2)+2.*YLC(1))/(XINC**2))
      PRE(2)=((4.*YLC(4)-YLC(5)-5.*YLC(3)+2.*YLC(2))/(XINC**2))
      DO 750 I=3,68
      P(I)=(-YLC(I+2)+8.*YLC(I+1)-8.*YLC(I-1)+YLC(I-2))/(12.*XINC)
      PRE(I)=((16.*YLC(I+1)-YLC(I+2)-30.*YLC(I)+16.*YLC(I-1)-YLC(I-2))/(
     &12.*XINC**2))
  750 CONTINUE
      DO 751 I=1,68
      XLC(I)=XI+(I-1)*XINC
      SHEAR(I)=DUMMYP(XLC(I))
      SPRE(I)=DUMMYL(XLC(I))
      WRITE(1,550) XLC(I),YINT(I),P(I),PRE(I),SHEAR(I),SPRE(I)
  550 FORMAT(1X,F7.3,2X,F12.8,2X,F7.1,5X,F8.1,11X,5X,F7.1,5X,F8.1)
  751 CONTINUE
      STOP
      END
C *************SUMROUTINE FOR MATRIX MULTIPLACTION*************
      SUBROUTINE MATMPY(A,B,C,M,N,L)
C     DETERMINES MATRIX C AS PRODUCT OF A AND B MATRICES
      DIMENSION A(15,25),B(25,16),C(15,16)
      DO 2 I=1,M
      DO 2 J=1,L
      C(I,J)=0
      DO 2 K=1,N
    2 C(I,J)=C(I,J)+A(I,K)*B(K,J)
      RETURN
      END
C     CHOLESKY SUBROUTINE FOR SOLVING EQUATIONS
      SUBROUTINE CHLSKY (A,N,M,X)
      DIMENSION A(15,16),X(15)
C     CALCULATE FIRST ROW OF UPPER UNIT TRIANGULAR MATRIX
      DO 3 J=2,M
    3 A(1,J)=A(1,J)/A(1,1)
C     CALCULATE OTHER ELEMENTS OF U AND L MATRICES
      DO 8 I=2,N
      J=I
      DO 5 II=J,N
      SUM=0.
```

```
      JM1=J-1
      DO 4 K=1,JM1
    4 SUM=SUM+A(II,K)*A(K,J)
    5 A(II,J)=A(II,J)-SUM
      IP1=I+1
      DO 7 JJ=IP1,M
      SUM=0.
      IM1=I-1
      DO 6 K=1,IM1
    6 SUM=SUM+A(I,K)*A(K,JJ)
    7 A(I,JJ)=(A(I,JJ)-SUM)/A(I,I)
    3 CONTINUE
C     SOLVE FOR X(I) BY BACK SUBSTITUTION
      X(N)=A(N,N+1)
      L=N-1
      DO 10 NN=1,L
      SUM=0.
      I=N-NN
      IP1=I+1
      DO 9 J=IP1,N
    9 SUM=SUM+A(I,J)*X(J)
   10 X(I)=A(I,M)-SUM
      RETURN
      END
```